HHS Public Access

Author manuscript

Anal Methods. Author manuscript; available in PMC 2018 June 13.

Published in final edited form as:

Anal Methods. 2017 ; 9(28): 4112–4134. doi:10.1039/C7AY00690J.

Surface acoustic wave devices for chemical sensing and microfluidics: A review and perspective

David B. Go[1,2,*], **Masood Z. Atashbar**[3,*], **Zeinab Ramshani**[2,3], and **Hsueh-Chia Chang**[2]

[1]Department of Aerospace and Mechanical Engineering, University of Notre Dame, Notre Dame, Indiana 46556, USA

[2]Department of Chemical and Biomolecular Engineering, University of Notre Dame, Notre Dame, Indiana 46556, USA

[3]Department of Electrical and Computer Engineering, Western Michigan University, Kalamazoo, Michigan 49008, USA

Abstract

Surface acoustic waves (SAWs), are electro-mechanical waves that form on the surface of piezoelectric crystals. Because they are easy to construct and operate, SAW devices have proven to be versatile and powerful platforms for either direct chemical sensing or for upstream microfluidic processing and sample preparation. This review summarizes recent advances in the development of SAW devices for chemical sensing and analysis. The use of SAW techniques for chemical detection in both gaseous and liquid media is discussed, as well as recent fabrication advances that are pointing the way for the next generation of SAW sensors. Similarly, applications and progress in using SAW devices as microfluidic platforms are covered, ranging from atomization and mixing to new approaches to lysing and cell adhesion studies. Finally, potential new directions and perspectives on the field as it moves forward are offered, with a specific focus on potential strategies for making SAW technologies for bioanalytical applications.

Graphical Abstract

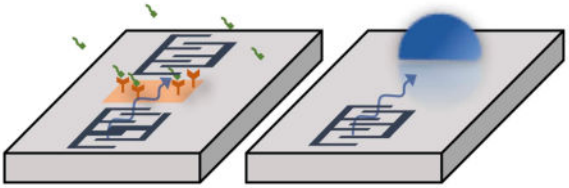

1. Introduction

The unique electro-mechanical coupling that occurs in piezoelectric crystals make them remarkably powerful materials. One particular use of piezoelectrics is to generate surface acoustic waves, often called SAWs, and like the material they originate from, these SAWs also have remarkable properties that make them useful for a variety of applications. Broadly,

*corresponding author: dgo@nd.edu; massood.atashbar@wmich.edu.

SAWs are mechanical waves constrained to the surface of an elastic material, with an exponentially decaying amplitude into the material bulk. SAWs can both occur in nature and be artificially engineered, and White and Voltmer's work on generating them using piezoelectric substrates in 1965[1] proved to be a technological breakthrough that laid the foundation for a variety of SAW-based devices. Since that time they have been widely used as components found in multiple modern electronics.[2,3]

But SAWs exhibit important characteristics that extend beyond electronic applications, and in particular, the last two decades have seen a variety of analytical technologies arise that capitalize on their unique properties. First, the mechanical vibrations are a strong function of their environment, including both their frequency and amplitude, and thus changes in the environment can lead to changes in the SAW itself. This forms the basis for a SAW sensor; target analytes change the SAW environment and changes in the SAW are subsequently detected. Second, the mechanical vibrations can be used as a mechanical actuator to induce a mechanical response in the environment. This is the basis of SAW-induced microfluidics; the SAW is used to actuate a liquid on the surface of the piezoelectric substrate, and this actuation is used for various analytical processes.

The focus of this article is to overview recent developments and trends in using SAW-based devices for sensors and chemical analysis. As this area has seen tremendous growth over the past two decades, there have been a number of good reviews, typically focusing on either SAW-based sensing[4,5,6,7,8] or SAW-driven microfluidics.[9,10,11] Our aim with this work is to overview developments in both areas, and focus on some of the more recent trends that have arisen in the past several years that are driving SAW-based chemical analysis technology. As these two areas have largely been distinct from each other, there are various potential opportunities to combine multiple SAW features to realize powerful, integrated analytic devices. It is within this context that we also propose possible directions for the field, with a specific emphasis on bioanalytical technologies, and look to the future of SAW devices in the analytical sciences.

This paper is organized into several sections. This introductory section covers the basics of SAW devices, how they are constructed, their common materials, and different operating modes. The two subsequent sections focus on SAW-based sensing (Section 2) and SAW-driven microfluidics (Section 3), respectively. We then offer our perspectives on future directions for SAW technology for chemical analysis (Section 4), including approaches where continued progress is needed as well as areas that are ripe for new developments. Finally, we conclude with some final thoughts (Section 5). For brevity, we omit extensive overviews of the history of both sensing and microfluidic fields as these have already been covered in the aforementioned reviews, although we do attempt to provide context for each area we discuss. Similarly, while we overview fundamental concepts in SAW sensing and microfluidic actuation, we point the reader to those reviews for detailed discussions.

1.1 Basics of SAW Devices and Operation

White and Voltmer[1] showed that piezoelectric crystals could directly produce SAWs when an interdigitated pair of electrodes on the piezoelectric surface is actuated by a radio frequency (RF) voltage (Fig. 1). The electromechanical coupling between the input electrical

single and piezoelectric crystal sends a traveling surface wave away from the interdigitated electrode. The amplitude of the SAW is on the order of nm and decreases exponentially into the bulk of the surface over a distance corresponding to roughly the wavelength (λ) of the SAW such that the energy in the SAW is highly localized at the surface of the substrate.[12] Additionally, depending on operation, the wave has both longitudinal and shear components, and for this reason it can effectively couple with different media (liquids, gas, particles) on the surface.

There are essentially three common modes of SAWs that are widely utilized in sensing and microfluidic applications. Perhaps the most general is the Rayleigh wave[13], in which the SAW propagates at the speed of sound of the crystal and the surface displacement has two components – one normal to the SAW propagation and one parallel (shear) to the substrate – resulting in an elliptical motion. While the Rayleigh wave mode can be used for gas sensing, it is also the primary mode used for microfluidic actuation as the Rayleigh wave refracts into liquid on the surface of the substrate, a phenomenon often called leaky SAW. The SAW then manifests itself as an acoustic pressure in the liquid, which can induce liquid motion called acoustic streaming, forming the basis for many microfluidic devices (Section 3) but posing challenges for liquid sensing where static liquids are preferred.[10,11] Similar to the Rayleigh wave is the Lamb wave[14], which are typically generated using very thin substrates that are only a few wavelengths thick.[15] Like Rayleigh waves, Lamb waves have both normal and shear components and can be used for gas sensing, but they are also well-suited for liquid sensing. Due to the low phase velocity of Lamb waves, there is no energy penetration inside liquid media placed on the SAW surface, and hence no acoustic streaming.

In the shear horizontal propagation mode, the particle displacement is only parallel with the substrate surface (there is no normal component) which inhibits vibration into any liquid on the surface.[16] Hence, like the Lamb wave, shear horizontal (SH-) SAWs cannot be used for microfluidic actuation, thus making them suitable for liquid-based sensing. Often times, a thin-film called a guiding layer is applied to the surface of the device to activate a Love wave mode[17], which also inhibits radiation of acoustic pressure into the liquid, making Love wave operation the most common for sensing in liquids.[18]

Importantly, the period and structure of the interdigitated electrode pattern, called an interdigitated transducer (IDT) or interdigitated electrodes (IDE), directly corresponds to the wavelength (λ) of the induced SAW as well as its propagation direction (Fig. 1a). The SAW device is operated at a designed resonant frequency (f) imposed by the IDT design, where in a typical IDT the electrode spacing is an integer multiple or 1/2, 1/3, or 1/4 of the wavelength $\lambda = 2\pi/k$, with k being the wavenumber. For most devices, the wavelengths are between 0.01 mm to 1.0 mm. A variety of IDT designs have been implemented to affect both the resonance and the propagation of the SAW. The most basic is a planar design, where the IDT consists of simple linear electrode ‘fingers’ and the interdigitated spacing is consistent for each finger pair, as shown in Fig. 1a. However, other clever IDT designs are possible, such as curved IDT configurations to produce focused SAWs[19] or variable-spacing ‘chirped’ IDTs that produce multiple resonant frequencies.[20] A single IDT design is generally used to generate planar traveling waves that propagate along the surface of the device, called a traveling wave, but sets of two or more opposing IDTs can also be used to

set up constructive interference and produce standing SAWs (Fig. 1b). To inhibit reflections and scattering off the edges of the SAW substrate and minimize wave reflection interference, acoustic absorbents such as gels are often applied to the edges of the piezoelectric substrate.[21] Ultimately, the IDT design depends heavily on the nature of the SAW device and the application in question, and for this reason a wide variety have been used.

As the development of SAW devices has matured, some particular operating parameters and materials have become common. For sensing applications, the SAW devices are typically at higher frequencies (~100–500 MHz) whereas most microfluidic devices operate at lower frequencies (~10–100 MHz). Similarly, the most common piezoelectric substrates are single crystal lithium niobate ($LiNbO_3$), lithium tantalate ($LiTaO_3$), and quartz (SiO_2) with common cuts including 128° *y*-*x* cut for $LiNbO_3$ and ST and AT cuts for quartz substrates. One of the most attractive features of SAW devices is that they are easily fabricated, generally requiring only modest spatial resolution (> 10 μm) and only surface microfabrication techniques. Further, they operate at relatively low powers (~1 W) and voltages (~10 V_{pp}). Together, their small size, high operational frequency, low power consumption, and compatibility with CMOS technology makes them particularly attractive for integrated sensing or microfluidic systems.[22,23] Further, with e-beam lithography on zinc oxide (ZnO) semiconducting films, GHz SAWs with wavelengths close to 1 μm can now be generated.[24] Hence, even though GHz is still far from electromagnetic wave frequencies, the wavelengths now do approach those of electromagnetic waves in air and liquid.

2. SAW-Based Sensors

2.1 SAW-Based Chemical Sensing Fundamentals

The principle behind SAW-based sensing devices is that chemical targets that adsorb on a functionalized surface on the SAW substrate fundamentally change the frequency of the SAW, and measurement of the frequency shift (Δf) can be correlated to the concentration of the target species. Based on this principle, SAW sensors were initially developed more than three decades ago[25,26], and are currently employed as fundamental components in a variety of microsensing systems.[8,18] The main advantage associated with SAW sensors is their high sensitivity and capability for the trace detection of a wide variety of chemical materials including bio/chemicals[27,28], organic and inorganic vapors[29,30], and explosives.[31] Furthermore, with continuous advancements in modern fabrication techniques, the development of miniaturized SAW sensors at relatively low costs is now possible.[32,33]

In general, a SAW sensing system consists of the SAW sensor, which is a sensing layer on the SAW substrate that is designed to react or bind with the analytical target, and electrical components designed for read out and recording the sensor output. The sensing layer interacts with the target to cause detectable changes in the features of the acoustic wave, such as the velocity or amplitude, which are then manifested as a frequency shift or insertion loss. As such, the sensing layer is a critical component of sensor design, and a wide variety of sensing layer materials have been explored for both chemical and biological SAW sensors. Polymers are one of the most common materials that have been used for SAW based gas sensing applications. For example, poly ethyl acrylate (PEA), poly epichlorohydrin (PECH) and poly isobutylene (PIB) have been used for the SH-SAW based

chemical sensing of fuel and oil in ground water.[34] However, polymer-based sensing layers are not preferred or are practically impossible for applications that operate at high temperatures due to their low mechanical and thermal stability.[35] This problem can be overcome by the use of semiconducting metal oxide-based sensing layers such as ZnO, CdO, SnO_2, TiO_2, CuO and WO_3.[36] Several nanomaterials such as silver nanoparticles[37], zinc oxide nanorods[38], carbon nanotubes[39], metal oxide nanowires[40,41], electrospun nanofibers[42] and palladium nanoparticles[43] have also been successfully used due to their high surface to volume ratio.[44,45] More recently, graphene oxide, which has a similarly larger surface area to volume ratio along with hydrophilic functional groups, has been used for humidity sensing applications.[46] For biological sensing applications, SAW-based sensors typically use various antigens as sensing layers and are deposited on the waveguide area. Some examples include the use of the hepatitis B surface antigen (HBsAg) for detecting the hepatitis B antibody in aqueous conditions[47,48] as well as triethoxysilylbutylaldehyde (ALTES) and triethoxysilylun-decanal ethylene glycol acetal (ACTES) for sensing influenza A viral antigens.[49]

As the piezoelectric crystal generates coupled mechanical and electrical fields, any changes in the environment (*i.e.*, sensing layer) that modulates either of these two fields, either a mechanical perturbation (*e.g.*, mass load) or acoustoelectric interaction (*e.g.,* conductivity change), is potentially detectable. Generally, the SAW propagation speed v is the speed of sound of the crystal, but changes in mass, stiffness, conductivity, dielectric coefficient, temperature and pressure can all modulate this propagation speed.[50,51] This change in propagation speed will proportionally shift both the resonant frequency f and phase ϕ of the SAW as[52]

$$\Delta v/v=\Delta f/f=-\Delta\phi/\phi. \quad (1)$$

Increasing the initial (unperturbed by the target) resonant frequency can enhance the sensor performance by increasing the frequency shift response and subsequent sensitivity. For this reason, SAW-based sensors typically operate at the higher end of the operational band (~100 MHz and higher) than most SAW-based microfluidics, which operate at much lower frequencies (~10–30 MHz). However, this has a practical limit as frequencies in the GHz range generate significant noise. Since the electric field is generated due to electromechanical coupling and polarization along the surface of the piezoelectric substrate, the sensitivity of the acoustoelectric interaction also depends on the electromechanical coupling coefficient (K^2) of the piezoelectric material. Piezoelectric crystals with high K^2, such as 36° YX $LiTaO_3$, are therefore generally more favorable for SAW sensors that are designed to perform based on a change in the electric field.

There are two common configurations for SAW sensors. The most basic is called a delay line configuration (Fig. 2a). Here, there is a first IDT that generates the SAW, which propagates through the sensing area, and the modulated SAW is subsequently detected by a second IDT, generating an electrical signal on the IDT.[53] The distance between the input IDT and readout IDT is the delay line, and the sensing layer is deposited in this region of the

substrate.[54] SAW delay line devices can be designed as one- or two-channel devices, where the latter consists of two SAW delay line devices fabricated parallel to each other. One of the channels does not have a sensing layer and thus acts as a baseline for the sensing channel.[55]

In the second configuration, to enhance the quality (*Q*) factor and decrease the impact of insertion loss[56], additional electrodes can be placed between the input and output IDTs as reflectors to create resonating cavities or 'resonators' (Fig. 2b).[57] The resulting resonant cavity minimizes scattering and confines the SAW energy into the substrate, improving performance. Like the SAW delay line configuration, the SAW resonators can also be used in single or dual channel[58], but rely on more precise IDT patterning to ensure reliability and repeatability.

2.2 Gas Sensing

Much of the success of SAW-based sensors has been for gas-phase targets, and a wide variety of sensors have been successful for both inorganic[59,60,61,62,63] (*e.g.*, hydrogen, ozone, nitrogen dioxide, etc.) and organic[64,65,66,] (*e.g.*, ethanol, methanol, toluene, chloroform, etc.) targets. The focus and effort in recent years has been on determining the best sensing layers for specific targets. For example, ammonia (NH_3) has received some attention of late. Hao et al.[67] explored different polymeric sensing layers on a $LiNbO_3$ SAW device for the detection of NH_3 including poly N-vinylpyrrolidone (PNVP), poly 4-vinylphenol (P4VP), polystyrene-co-maleic anhydride (PSMA) and poly-capro-lactone (PCL). Generally, larger frequency shifts, and thus greater sensitivity, were demonstrated for P4VP and PNVP polymer films, and this was attributed to hydrogen bonding between the polymer and target. Another study, by Raj et al., investigated the cross-sensitivity and selectivity of SAW sensors towards NH_3 with other common volatile organic compounds (VOC).[68] Rather than using a polymer sensing layer, they looked at varying thicknesses (20, 40, 80 and 100 nm) of zinc oxide (ZnO) films on SAW resonators. They concluded that the SAW sensor was more sensitive toward liquid and gaseous NH_3 when compared to methanol, ethanol, acetone, benzene, xylene, water vapor, nitrous oxide and hydrogen. It is worth noting that the frequency shift Δf was positive for liquid NH_3, while Δf was negative for the other VOCs, thus demonstrating selective detection. Finally, Tang et al. developed SAW sensors based on Co_3O_4/SiO_2 and ZnO/SiO_2 composite nanofilms on ST-cut quartz substrates for the detection of NH_3 gas.[68,69,70] Both individual and composite films were tested, and generally higher sensitivities were obtained with the composite films, with a demonstrated detection limit of 30 ppm at a 2 kHz frequency shift and 1 ppm at a 3.5 kHz frequency shift for the ZnO/SiO_2 and Co_3O_4/SiO_2 composite nanofilm structures, respectively.

The nanocomposite strategy for the sensing layer has, in general, begun to receive more attention as it often leads to increased sensitivity. Sayago et al.[52] explored polymer-based sensing layers, comparing nanocomposites based on polyepichlorohydrin (PECH) and polyetherurethane (PEUT) with different percentages of multi-walled carbon nanotubes (MWCNT) (Fig. 3). The nanocomposites were employed as sensing layers on ST-X cut quartz SAW sensors for the detection of VOCs such as octane (C_8H_{18}) and toluene (C_7H_8) in the presence of hydrogen (H_2), nitrogen dioxide (NO_2), carbon monoxide (CO), and NH_3.

The introduction of MWCNTs was particularly notable as it made the device selective to toluene and octane, with no response observed for interfering gases. Further, the introduction of MWCNT into the polymers only increased the sensitivity of the device toward toluene (Fig. 3c).

VOCs in particular have been a focus of much of SAW sensor design over the last decade due to their potentially harmful impact on human health and the environment. Meulendyk et al. offered a slightly different take on this by developing a SAW sensor for hydrogen fluoride (HF), which is typically a decomposed product of several VOCs and is also used in different industrial processes.[71] Their study compared both a generalized SAW ST-X quartz resonator and a SH-SAW ST-90° quartz resonator. Notably, the shear-horizontal SAW device displayed frequency shifts up to 4.6 times greater than the general SAW resonator, directly correlating to a better sensitivity. This study also showed that the frequency response to other potential interfering compounds such as tetrafluoroethane, isopropanol, propane, acetone, and carbon monoxide (CO) was below the device's detection limit of 0.8 ppm. The detection of chemical warfare agents (CWA) using SAW sensors as a so-called electronic nose (E-nose) has also been of interest. Raj et al.[72] developed SAW sensors for the detection of CWAs by employing four different oxides as sensing coatings and tested four different CWAs. As shown in Fig. 4, they demonstrated the capability of their E-nose to detect and differentiate among the vapors of the CWAs at concentrations down to single digit ppm, with SnO_2 showing the greatest sensitivity for each agent.

Although there is still much work to improve performance, SAW-based gas sensors are the most mature of the SAW chemical sensors, and their high sensitivity makes them competitive in the market place. SAW-based gas sensors have been widely implemented for the detection of chemicals, explosives and drugs in commercial applications including emergency response, gas detection, and laboratory analysis.[73,74,75,76] Parker Hannifin offers the Trihalomethanes (THM) Analyzer, which uses SAW detection technology for ppb-level sensing of various chemicals, including chloroform and bromoform, in approximately 30 minutes.[73] Sandia National Laboratories developed μChemLab™, a gas analysis system that uses SAW sensors for the detection of benzene, toluene, octane, and xylene in 5 to 10 minutes at ppb sensitivities.[74] Biosensor Applications® offers the portable BIOSENS®300 and BIOSENS®600 systems for drug and explosive detection.[75] These systems are capable of detecting around 30 chemicals including Trinitrotoluene (TNT), 2,4-Dinitrotoluene (DNT), Research Department Explosive (RDX), Pentaerythritol tetranitrate (PETN), Nitroglycerin (NG), Meth-amphetamine, amphetamine, cocaine and heroin/opiates with a response time of 30 minutes and ppb detection limit. The fully portable 4300 zNose from Electronic Sensor Technology, Inc. can detect and analyze explosive vapors of TNT, triacetone triperoxide (TATP), composition-C4 and NG.[76] Even though this system also provides ppb detection limit, it has a much lower response time of 5–60 seconds and thus has advanced capabilities when compared to that of the BIOSENS®300 and BIOSENS®600 systems.

Even though several SAW sensor-based portable systems are commercially available for gas detection applications, further research focused on extending the sensor performance would be useful. For example, advances in modern technology have enabled the use of trace

amounts of chemicals in several industrial applications. In addition, both drugs and explosives are being stored, transported, and used in novel methods that are often untraceable. Moreover, the typical vapor pressure of an uncontained explosive mass, in air, can be in the part per quadrillion (ppq) range.[77] Research has shown the capability of SAW sensors to detect trace amounts of gases with detection limits as low as parts per trillion (ppt).[78] However, commercial gas sensor systems with these high sensitive SAW sensors are not yet available. Therefore, the development of novel miniaturized, real-time, and portable SAW based systems for commercial use with higher sensitivities (ppt and ppq) along with faster response times (5–10 seconds) is desirable.

2.3 SAW-Based Liquid and Biological Sensing

In addition to gas sensing, liquid sensing has also seen significant interest, with a particular focus on biological targets. Conceptually, the approach is not that different from gas sensing, although there are practical challenges. For example, corrosion of the IDTs can be a challenge, and some strategies include adding an additional polymer layer over the IDTs for protection. Additionally, the high permittivity of the water buffer reduces the localized electric field of the SAW wave and hence diminishes its amplitude. The initial compression of the SAW with a normal displacement also involves significant leakage into a liquid such that the SAW wave amplitude attenuates very rapidly, even if the waves are generated in a mode so that refraction into the bulk does not occur. Devices that can generate SH-SAWs, with much less bulk leakage, began to appear in the 1990's, and many use a Love thin-film wave guide to further prevent leakage into a liquid on the surface.[79,80,81,82]

Knodoh *et al.* demonstrated using a shear horizontal approach by detecting various types of Japanese tea, monitoring both frequency shift and amplitude change.[83] Since then, the applicability of shear horizontal has been expanded, including oil contamination[34] and heavy metals[84] in ground water. The latter study by Ramshani et al. took advantage of modern fabrication techniques to develop a cost efficient and easy-to-use flow cells for heavy metal compound sensing (Fig. 5).[84]

To use SAW devices as biosensors, antibodies or receptors are attached to the sensing layer to bind with target antigens. To prevent unspecific binding in label-free detection methods, as well as retain the functionality of the trapped molecules and facilitate binding, hydrogel layers such as dextran are used to cover the sensor surface. While literature provides an extensive amount of information about the vast range of targets and proven sensing materials combinations that can be used in SAW sensors, discriminating between these can often be difficult. Verma and Yadava recently proposed using data mining algorithms such as fuzzy clustering to guide polymer selection for specific targets, validating their work with simulated sensor performance.[85] Although they did not focus on specific biotargets, instead exploring vapor by-products from biological processes, their work provides a unique way to utilize the availability of data to advance sensor design.

To date, a wide variety of biological targets have been studied, including proteins[86,87], DNA[88], and large cells and bacteria[89,90,91,92], as well as biological warfare agents (BWAs)[93] and aflatoxins.[94] From a diagnostic and therapeutic perspective, there are multiple approaches that have been explored. Csete and Hunt, for example have proposed SAW-based

biosensors for the early detection of sepsis, with the focus being detecting NO, rather than a biological target, in human breath.[95] Chang et al. proposed a label-free diagnostic SAW device for monitoring cyclosporine A (CsA), an immunosuppressant therapeutic drug, in whole blood for therapeutic drug monitoring in, for example, organ transplant patients.[96] The device demonstrated about 3 orders of magnitude dynamic range and a limit of detection down to 0.89 ng/mL. At a total throughput detection time of 40 min and reuse up to 10 times on clinical samples, they demonstrated the potential applicability to the device in a clinical setting. The same group also develop a SAW-based sensor for detecting circulating cancer cells (CTCs), with the same benefits in speed and reusability.[89] Focusing on human breast cancer cells, and specifically MCF-7, they placed aptamers on their sensing layer, using a multi-channel approach where a known sequence targeting the mucin 1 protein on the MCF-7 cell was attached to the detection channel and a random sequence to the reference channel. In optimized conditions, they showed a 5 order dynamic range and a limit of detection of 32 cells/mL. Liu et al. took advantage of the properties of graphene to include graphene oxide (GO) on their sensing layer rather than a polymer like dextran for a SAW biosensor for the detection of various polymorphisms in the enzyme cytochrome P450 2D6 (CYP2D6).[88] Although they do not specify the exact reason for the enhanced performance, they did observe better sensitivity with the GO-enhanced device over dextran. Perhaps more importantly, they demonstrated clinical utility by differentiating polymorphisms in over 130 clinical samples.

Despite such successes, the development of sensitive and selective SAW sensors for biomolecular detection remains challenging. For DNA detection, for example, the targets are typically long (200 bases) with a high dissociation constant of 200 nM.[88] There are much cheaper (potentially disposable) biosensors that can achieve better sensitivity (with a dissociation constant of 200 pM for 20-bp targets).[97] However, SAW sensors have been shown to be highly selective, and single-nucleotide and multi-site polymorphism discrimination has been reported by several researchers.[88,98] This selectivity is impressive, as thermodynamic dissociation constants for mutants and wild types of this length should be experimentally indistinguishable. This suggests that the SAWs can kinetically shear off debris in the solution and non-specific bound non-targets from the probes, which are relatively abundant in untreated physiological samples. There is growing interest in how to tune such external forces to enhance selectivity by irreversible kinetic dehybridization to overcome thermodynamically indistinguishable targets.[99,100,101] SAW-based devices, however, appear to achieve such selective dehybridization without external flow or an external field. Conceptually, there should be an optimum operating voltage, and corresponding SAW amplitude, for each target that can dehybridize non-targets but not the targets. A detailed study of SAW selectivity enhancement would be an interesting new direction, and could prove to be an attractive feature that helps SAW-based biological sensors overcome their limited sensitivity.

2.4 Advances in Device Fabrication

Advances in fabrication techniques have also found their way to SAW sensors. Some of these have been employed in the aforementioned studies above, and here we highlight a few specific ones that show significant promise in transitioning SAW sensors into marketable

devices. In particular, recent efforts have focused on developing novel flexible substrates that do not employ conventional, rigid single-crystal piezoelectric substrates. Jin et al. developed flexible SAW devices by depositing ZnO nanocrystals on bendable Kapton polyimide films (Fig. 6a).[102] The flexible SAW devices exhibited two wave modes – the Rayleigh and Lamb wave modes with resonant frequencies of 198.1 MHz and 447.0 MHz, respectively and signal amplitudes of 18 dB. The fabricated SAW device was also successfully used for acoustic streaming inside a liquid droplet (Fig. 6b), thus demonstrating its potential for chemical analysis in lab-on-chip applications such as those discussed in Section 3. Li et al. also developed flexible SAW devices by direct current reactive magnetron sputtering of *c*-axis oriented aluminum nitride (AlN) films on polyimide substrates (Fig. 7).[103] They were able to fabricate a functional delay line device, but it had high insertion loss. They suggested this could be overcome by adding a transition layer or simply by design optimization. Perhaps more importantly, wearable sensor technology continues to grow in popularity, and these types of SAW devices that have flexible and conformal form factors have the opportunity to play an important role in the field.

In addition to flexible substrates, novel concepts using conventional substrates continue to emerge. The advent of additive manufacturing techniques for rapid prototyping of electronic devices have seen some people focus on the use of printing processes for the fabrication of SAW devices. Roshanghais et al. developed a novel device where they integrated a standard $LiNbO_3$ SAW resonator chip into a 3D-printed SAW transponder housing that had inkjet-printed wireless antenna and contact pads using silver nanoparticle ink.[104] The functionality of the fabricated device was investigated by wirelessly interrogating it with a CTR frequency-modulated continuous-waveform radar reader unit. There has also been development on microelectronic circuits for use with SAW based chemical sensors. Cenni et al. designed a 0.35 μm CMOS technology-based microelectronics front-end interface for integration with a SAW sensor that could be used to detect the concentration of environmental gaseous mercury.[105] Simulation results demonstrated a 0.2 ppm resolution for the SAW sensor. This model could thus be employed practically for detecting gaseous mercury concentration changes by embedding the SAW device in a phase-locked loop (PLL) for conversion into frequency shifts.

In summary, all these advances show that it is possible for SAW devices to evolve beyond the standard piezoelectric crystal configurations that have been the most prevalent over the past 20 years. In order to realize SAW sensors that can be truly be widely adopted by industry, both new strategies for high volume manufacturing and novel form factors, such as flexible devices, will be needed.

3. SAW-Integrated Microfluidics

As noted above SAW-based sensors, especially for biological targets, often operate with liquid on the surface of the SAW device. In fact, the mechanical interaction of SAWs with liquids can lead to unique behaviors that can be used not only for direct sensing, but fluid manipulation ranging from induced mixing and sorting to the generation of aerosols. A SAW microfluidic device can then be used in conjunction with other sensing and detection technologies to enable the analysis of minute volumes of liquid sample.

While early studies established the basic theoretical foundation of acoustic streaming and atomization[11], over the past several years, fundamental understanding for SAW-fluid interactions has continued to grow. Like non-dispersive bulk electromagnetic waves, both compression and shear SAW waves can be described by a ray theory for analogous phenomena like refraction when they travel from one medium to another with a different wave speed. Indeed, when a gas-solid SAW wave propagates into a liquid medium, part of it is refracted into the bulk liquid phase at the Rayleigh angle (ϕ) relative to the normal of the solid surface

$$\phi = \sin^{-1}(c_s/c_l), \quad (2)$$

where c is the speed of sound, and the subscript s correspond to the solid and the subscript l denotes liquid, respectively. This speed of sound is related to the elasticity E of the piezoelectric crystal by $c_s = (E/\rho_s)^{1/2}$. Much like the evanescent electromagnetic waves of a reflected or refracted optical wave, there is also an exponentially decay SAW wave component that is transmitted along the liquid-solid surface and is not scattered into the liquid bulk. The decay length of this evanescent SAW wave is

$$L = (2\pi\rho_s c_s)/(k\rho_l c_l), \quad (3)$$

where k is the wavenumber and ρ is the density of the medium. The decay length is much larger than the SAW wavelength by a factor equal to the ratio of $(E/\rho_s)^{1/2}$, but is still on the order of several mm at most. For GHz SAW waves, L could be as short as 10 to 100 μm.

The refracted SAW wave into the liquid bulk can induce multiple phenomena in the liquid (Fig. 8). Primarily, the acoustic pressure produces a streaming effect as shown schematically in Fig. 8a; if the liquid 'bulk' is a droplet on the surface of the SAW device this streaming can cause the droplet to translate (move laterally) if the SAW is a traveling wave or simply vibrate if the SAW is in a standing wave configuration (Fig. 1b). A number of fundamental studies have focused on understanding this particular behavior[106,107], and recently Rezk et al. showed that fingering instabilities can arise under some conditions, leading to soliton-wave like propagation of liquid fingers away from the droplet.[108] In addition to bulk liquid motion, the streaming effect also forms capillary waves on the surface of the liquid and can lead to the breakup of the droplet or a liquid film to form jets, large drops, or microscale drops (atomization or aerosolization). Tan et al. showed that the mode of this breakup depends on the relative size of the liquid film or droplet on the SAW substrate to the frequency of the SAW, isolating these different regimes as shown in Fig. 8c.[109] Importantly, as discussed in the ensuing sections, these different regimes can be used for different microfluidic applications.

One of the more interesting approaches to SAW microfluidics is coupling the SAW device with a fibrous wick such as paper or thread to continuously deliver solution to the SAW surface from some external reservoir as shown in Fig. 8b. As opposed to a single droplet on

the SAW substrate or solution delivery from a capillary pump or similar, paper wicking allows continuous solution (and thus sample) to be brought to the SAW surface with no external pumping source. Such an approach is attractive when using these devices in portable and/or low-resource conditions, where electrical power delivery is at a premium. Practically, this has been shown to be useful for multiple applications (Section 3.2), but it also introduces interesting fluid dynamics. At the contact point between the end of the wick and the substrate, a thin film of fluid is extracted onto the surface of the SAW substrate. Unlike a surface droplet, the extracted film has a decaying film thickness and is continuously replenished as it loses fluid to evaporation and/or atomization. This extracted film serves, in effect, as a “pinned” droplet that is unable to translate and has a much different contact line than a typical droplet.

Rezk et al. noted that if the solution was atomized from the thin film, the SAW acted to pump solution from the reservoir through the wick.[110] This pumping action is much faster than the natural pumping action due to capillary pressure alone. Taller et al. looked at the atomization from the leached thin film to reveal that the profile of the thin film changes due to the radiated SAW pressure.[111] In addition to showing different atomization regimes as shown in Fig. 9, they also estimated the internal pressure in the thin film for each of these regimes, and importantly it can be negative. This negative pressure, especially during rapid atomization (Fig. 9c), produces a strong positive pressure gradient through the wick causing a pumping action with linear flow velocities approaching 1 mm/s. Interestingly, at low SAW amplitudes, the thin film does not atomize but instead breaks up into a series of small surface satellite droplets with characteristic sizes that decay exponentially from the paper wick (Fig. 9a, inset). [112] In fact, two families of droplets were observed – larger ones (> 10 μm) sustained by the acoustic pressure, but also surface droplets as small as ~200 nm due to the electrostatic pressure from the SAW evanescent wave that continues to propagate along the substrate surface. Taller et al. estimated that the electric field within this evanescent SAW wave exceeds 10^6 V/cm, roughly sufficient to break up certain bonds like in for water splitting[113] as well as ionize analytes in the droplet, which can be used for mass spectrometry.[114,115]

Ultimately, this fundamental behavior can be capitalized upon to design a variety of microfluidic devices – from those that take advantage of the bulk acoustic pressure to capture, pattern, and manipulate particles to others that capitalize on the large electric fields to induce lysing or ionized aerosols. Like SAW sensors, SAW-based microfluidic devices can take many forms, and Table 1 shows a broad overview of devices that have emerged over the past decade. The following sections highlight some of the more specific advances useful for chemical and biological analysis.

3.1 Sprays and Aerosolization

Using SAWs to generate sprays and aerosols has been known for nearly two decades, with some of the earliest papers dating back to the mid 1990s and beginning of the 21st century.[125,126,127] As discussed above, there have been a large number of studies focused on a fundamental atomization mechanism, and much of the focus of recent work has been on engineering SAW atomization devices.[128,129,130] Further, some novel new applications have

been developed including spray cooling[131] for thermal management, spray coating[132,133], and even aerosolizing particles to load an optical trap.[134] However, in terms of chemical analysis and lab-on-a-chip applications, two primary applications have emerged and grown to near maturity.

One of the first proposed applications was by the groups of Yeo and Friend to generate micron-size aerosols for pulmonary drug delivery[135], and this is now close to being a commercial product. In addition to advancing the miniaturization and portability of a SAW-based nebulization platform[136], the groups have also focused on the viability of the atomized species, to ensure there is no SAW-induced degradation or similar integrity issues. To that end, the group has explored various shear-sensitive medicinal targets, including epidermal growth factor receptor (EGFR) monoclonal antibodies, antimicrobial peptide antibodies, plasmid DNA, and even stem cells to treat lung cancer and lung disease.[137,138,139,140]

Around the same time as pulmonary devices were first introduced were the first reports of using SAWs to produce charged droplets for mass spectrometry, where ionized analytes are transferred from a droplet on the SAW surface to the inlet of a mass spectrometer.[114,115] Critical to this application is that the ionization is ‘soft’, meaning that large biomolecules (*e.g.*, proteins) are not fragmented during the ionization process. Qi et al., for example, showed that intact proteins and cells could be aerosolized this way[141], and Huang et al. has specifically shown that ions produced by SAW atomization have lower internal energy than electrospray ionization.[142] The Goodlett group in particular have pushed to make SAW-based atomization (which they call SAWN – surface acoustic wave nebulization) a viable alternative to conventional mass spectrometry ionization sources[114,142,143], including developing specific chemical analysis methods (*e.g.*, lipid identification)[144,145] as well as optimizing and advancing SAW device technology (*e.g.*, using standing wave configurations).[146,147,148] One particular limitation of SAW MS compared to more established techniques such as electrospray ionization (ESI) is interfacing with upstream separation techniques, such as liquid chromatography (LC). Tveen-Jensen et al. have recently successfully demonstrated the coupling the of LC with SAW MS (Fig. 10), although they note that the LC capillary needs to be at an optimal location on the SAW device, which adds an element of complexity, and that there is more variability to the SAW data when compared to ESI.[149]

One of the more clever aspects of Ho et al.’s original study was how they integrated paper sample delivery to the SAW device, where filter paper wicked analyte solution from a reservoir to be directly atomized by the SAW device, similar to the configuration shown in Fig. 8b.[115] The paper acted as a natural filter, allowing for the direct analysis of raw biological samples with little pre-treatment. They were able to showed they could analyze both raw blood and plasma samples and detect target analytes (in their case, pharmaceuticals) in the sub-10 nM range, with no pre-treatment except minimal dilution of the raw sample. Most of the large bioparticles, such as blood cells, were simply collected in the paper wick, which could then be easily disposed.

3.2 Microfluidic Sorting, Separating, Mixing, and Concentrating

Analytically relevant technologies have also taken advantage of the induced streaming by SAW waves, whether that be in droplets or microfabricated microchannels. Over the past several years, there has been an abundance of growth in using SAW devices for the manipulation of fluids, or relevant particles in the fluid, through mixing, concentration, and sorting and separation. While SAW often does not provide the detection technique itself, it provides an effective, low-power, and relatively simple means of conducting many of the upstream steps necessary for effective analysis.

One of the areas where there has been some remarkable demonstration of the capability of SAW has been in separation and sorting technologies. Some of the earliest reports of naturally occurring separation began appearing around 2008, when Alvarez et al. showed that using two sets of IDTs opposing each other created a standing wave; this standing wave naturally broke up a polymer liquid film into a periodic array of droplets[150], similar to the effect shown in Fig. 9a[112], where the droplets form at the nodes of the standing wave. Huang's group capitalized on this effect to sort cells and particles in a channel and isolate them into specific patterns, calling their technique acoustic tweezers or the acoustic analog to optical tweezers.[151,152] The mechanism of the sorting is that the standing wave creates localized acoustic pressure nodes and a differential pressure field, and this pressure field establishes unbalanced acoustic forces on particles, leading them to migrate toward the nodes or antinodes of the standing wave and subsequently become trapped. Sorting design, therefore, is in large part based on configuring the nodes of the standing wave through IDT design (Fig. 11). Several key things stood out from this work. First is that the approach could be used to not only rapidly (< 1 s) separate particles with high efficiency (>80%) in a bulk solution, but also using a flowing microchannel, making it readily suitable as an upstream device for a downstream detection method. Second, the technique also naturally concentrated the target particle, also making it a valuable upstream sample preparation technique. Finally, the only major force exerted on the particles was a shear force, meaning that the effect was independent of the particles' optical, electrical, or magnetic properties, in contrast to optical or electromagnetic/kinetic sorting technologies.

Huang's group has subsequently expanded on this technique and applied it for a number of specific biological targets ranging from cells and platelets to protein crystals and entire organisms, showing little loss in biological viability. [10,153,154,155,156,157,158,159,160,161,162] Much of this work has focused on developing clever IDT designs, including chirped IDTs that allow for multiple resonance frequencies[10] and tilted-angle IDTs that allow for better control of the separation. [154] One particular advancement was integrating fluorescent labeling and a fluorescence detector to developed a feedback-controlled method for rapid sorting – a so-called fluorescence activated cell sorter (FACS) – that allowed for the selective separation of cell targets from a heterogeneous sample.[161,162] However, integrating FACS is not always necessary, as the SAW-based separation is inherently dependent on the size/shape/density/compressibility of the target cell, and thus there can be *in situ* sorting simply based on cell type.[154] Recently, they demonstrated this on clinical samples, separating circulating tumor cells (CTCs) from white blood cells in whole blood at a sample throughput rate of about 1.2 mL/hr (Fig. 12), and demonstrated the potential for biomarker

detection by analyzing the blood from three breast cancer patients at different stages of cancer development.[158] Along those lines, much of the recent focus has been on applying SAW separation to more clinically-relevant conditions, including platelets and bacteria from whole blood [153,159] and inflammatory cells from sputum.[160] While Huang's group has been the most prolific in this area, others have also contributed[163,164], demonstrating, for example, SAW-based separation within a surface droplet[165] or using a traveling wave approach, rather than a standing wave.[166]

Similar to sorting technologies, a variety of SAW-based mixing and concentrating technologies have been developed over the past several years, taking advantage of the induced acoustic streaming. Sample pre-concentration can be a vital step in many analytical methods, especially when considering the minute concentrations of target analytes encountered in many biomedical media (*e.g.*, blood), but is often difficult to do at the small scales of microfluidics.[11] To that end, SAW-based technologies have shown significant promise.

Two of the earliest reports came out of the groups of Yeo and Friend.[167,168] Li et al.'s work was particularly interesting as they demonstrated SAW-induced concentration by using various strategies to break the symmetry of the planar SAW, inducing rotational motion within a droplet (Fig. 13).[167] This concept of microcentrifugation has been the foundation of multiple studies since that time, using a wide variety of IDT and device designs for both standing and traveling wave SAWs to break the symmetry and induce mixing and concentration[19,117,118,169,170,171] ultimately yielding a lab-on-chip technology Glass et al. called 'miniaturized lab-on-a-disc (miniLOAD)'.[172] The miniLOAD device integrates a SAW microcentrifuge with a rotating disc containing multiple microchannels, essentially creating the opportunity for mixing in isolated or connected microchambers

One of the first studies showing the utility of this SAW micromixing used SAW microcentrifugation to accelerate protein processing in gels, including tryptic digestion and peptide extraction, reducing the time from sample preparation through analysis to only ~30 min.[173] More recently, Alhasan et al. used SAW microcentrifugation to assemble cellular spheroids from loose cell aggregates; cellular spheroids are three-dimensional cell structures that more closely mimic cell-cell and cell-matrix interactions found in *in vivo* environments.[174] Using a clever quick-gelling hydrogel coupling layer, the SAW device was integrated with a microwell plate that contained suspensions of cancer cells (mammary gland carcinoma). As the SAW microcentrifuge concentrated the suspended cells in the center of the microwell, they were able to form tight spheroids without losing cell viability, rapidly producing a platform to study fundamental cell-cell interactions.

As most microcentrifuge approaches are for batch approaches using a fixed liquid volume (*i.e.*, droplet or microwell), new strategies are emerging for continuous flow mixing.[175,176] This offers additional challenges as the bulk flow can decrease the residence time in the mixing region, which subsequently decreases the mixing intensity and/or concentration effectiveness. Recently, Gracioso Martins et al. used this approach to design a fully miniaturized flow injection analysis-chemiluminescence (FIA-CL) system with an integrated, on-board-powered SAW microcentrifuge (Fig. 14).[177] Using a pulsing strategy

(~2 Hz, 25%–75% duty cycle), they could increase the SAW amplitude and enhance mixing, and with suitable optimization they demonstrated a SAW-enabled FIA-CL device with a limit of detection of 0.02 ppd for the target L-proline, about two orders of magnitude better than conventional, benchtop FIA. Similarly, Chen et al. used a standing SAW device to develop a microfluidic cytometer.[178] Using dual IDTs, they induced a three-dimensional focusing field that concentrated analytes in a continuous flow microchannel. Downstream of the focusing section, the analytes were interrogated using laser induce fluorescence (LIF), and using both model particles and leukemia cells, demonstrated enhanced detection. Mao et al. recently showed a similar approach for concentrating nanoparticles within the center of flow through a glass capillary, and using these nanoparticles to capture fluorescently-labeled bioparticles (*e.g.*, streptavidin) made for an integrated concentration/detection strategy.[179] Along those lines, Westerhausen used a microchannel mixing strategy to synthesize mono-nucleic acid/lipid particles (mNALPs) by mixing separate liquid streams of lipids and nucleic acids in what amounted to a solvent exchange process.[180]

In addition to these more conventional microfluidic approaches, other unique concentration and mixing strategies have also been developed. For example, Zhang et al. simply used the ability of SAW to translate droplets to merge and mix them.[181] Rezk et al. took advantage of paper-based sample delivery and SAW atomization (*e.g.*, Fig. 8b) and developed a paper-based mixing strategy.[110] As the atomization extracts liquid from the paper and induces pumping, multiple fluid streams can be combined, which can be used to either mix analytes or create a concentration gradient. Ramesan et al. expanded on this concept by using cotton thread rather than paper as the sample carrying medium.[182] Using a mesh or network, they could create different channels and produce a concentration gradient from two supply solutions throughout the network (Fig. 15). Further, once the concentration gradient is set, it can be ‘frozen’ in place by placing the entire thread network in a hydrogel. This creates a thread network that can be designed to represent a tissue microenvironment such that it can be used to conduct chemotaxis studies. Ramesan et al. demonstrated this, in principle, by seeding the thread network with cells and exposing the network to nutrient gradients to test cell viability. As both paper- and thread network-based chemical platforms are seeing increasing popularity due to their low cost and low power, the integration of SAW devices is one strategy to enhance these techniques without a significant sacrifice in portability or power.

3.3 Lysing and Other Microfluidic Manipulations

While microfluidic applications in atomization, separations, and mixing have all continued to grow since the first studies came out nearly a decade ago, new uses of SAW microfluidics have started to emerge more recently. In particular, the induced acoustic shear forces as well as electric fields have been revealed to induce lysis of bioparticles. In 2012, two groups showed the first evidence that SAW could induce lysis in cells. Lyford et al. conducted one of the first studies, demonstrating the lysis of Gram-positive bacterium Geobacillus thermoglucosidasius in a surface droplet by a delay-line SAW device configuration.[183] They found an interesting coupling between SAW lysis and sample temperature, showing the process to be generally inefficient at 5°C, plateauing at only 10% lysis after nearly 8 min. Heating the sample improved both the rate of lysis and the lysis efficiency, reporting an

efficiency of 30% for temperature at 30°C. The general trend showed even higher temperatures were more rapid and more efficient, but droplet evaporation limited the applicability.

The group of Cooper introduced the concept of phononic crystal structures for SAW-based manipulation, where they bond a SAW substrate with a disposable superstrate that has a micromachined periodic lattice (Fig. 16a). The phoninic lattice can be designed to act as a filter or waveguide for the SAW wave, and when coupled with the position of the superstrate, can facilitate a wide variety of microfluidic behavior – from microcentrifugation to nebulization.[184,185,186] Using this concept, Reboud et al. reported an integrated SAW-driven phononic chip that could both induce cell lysis to release internal DNA and subsequently conduct on-chip PCR to immediately detect DNA targets, focusing on detecting malaria.[187] This study was an important step because it revealed the inherent utility of on-chip SAW lysis – the easy coupling with other microfluidic manipulations. As conventional chemical lysis involves detergents and enzymes, subsequent analysis typically requires additional washing and purification steps, such as centrifugation. SAW mechanically lyses the cells, so no cleaning or washing steps are required, not only accelerating and simplifying the entire analysis workflow but facilitating integrated on-chip devices where cells and other bioparticles are maintained within their physiological buffer. The same group recently followed up this study with a method to differentially lyse human cancer cells and then detect the released proteins using an antibody-capture strategy and total internal reflection (TIRF).[188] Unlike their earlier study, this was not all done on the same chip, but on two separate chips, although the potential for complete integration is still there. From a lysing perspective, they found that it was necessary to break the symmetry of the planar SAW wave and induce vorticial motion (à la microcentrifugation) to generate sufficient shear to lyse the cells (Fig. 16). Increasing the SAW power generally improved lysis, but was limited by both atomization and heating of the SAW chip to evaporate the droplet, and thus they incorporated 10 μm polystyrene beads to help break the cell membrane at low SAW powers. As suspected, the beads helped to lyse the cells, likely through a grinding effect, and more importantly, parameters could be further tuned to either break the cell nuclei or leave them intact.

Taller et al. have taken the lysing approach one step further, targeting not ~10 μm cells, but the much smaller ~10–100 nm exosomes that are released by cells.[189] Exosomes are microvesicles secreted by cells carrying a variety of messenger (mRNA) and microRNA (miRNA), and are currently understood to be a major player in cell-to-cell signaling. As cancer cells are known to release many more exosomes than healthy cells, profiling of their miRNA cargo may allow detection of irregularly expressed miRNAs specific to particular cancer cells, and thus may prove to be a more reliable biomarker than other strategies.[190] Like others[188], Taller et al. included a separate, downstream detection strategy for the released miRNA consisting of an ion-exchange membrane sensor, but unlike others[183,187,188], they integrated the SAW device with a continuous flow microfluidic channel. As opposed to single microdroplet lysing, this allows for continuous lysing of the sample and the potential for high throughput. In fact, when coupled with their ion-exchange membrane sensor, they were able to show detection of target miRNA in cancer cell media down to pM concentrations with the workflow reduced from > 12 h to approximately 1.5 h.

The mechanism for exosome lysis, however, is unclear. Cell lysis is almost certainly due to the strong shear forces induced by acoustic streaming, but as exosomes are ~1/1000 the size of cells, it is not clear that shear forces are responsible at the exosome scale. As discussed above, the evanescent wave of the SAW induces surface electric fields that can penetrate several μm into the solution, and Taller et al. estimated the magnitude of the field to be ~10^6 V/m.[112] It is likely that these fields are responsible for the lysing action, and the ~40% efficiency they reported can be improved upon by both shaping this electric field and designing microfluidics to ensure strong contact between the exosomes and the field.

One unique application that has also emerged is based on the principle of using SAW streaming to shear cells from a surface, thus creating a platform that takes advantage of the adhesive properties of cells to specific surfaces. Hartmann et al. called their tool a De-Adhesion Number Investigator (DANI) and showed a thorough initial study of the de-adhesion of SAOS-2 cells.[191] For example, as shown in Fig. 17, they were able to characterize the adhesion/de-adhesion from various substrate types, including titanium (Ti), Ti covered with diamond-like-carbon (DLC), and Ti-covered DLC with silver nanoparticles embedded as an antibacterial mimic (Ag:PVP). They argue that they can derive both the initial adhesion affinity and de-adhesion rate from their platform, making it well suited to study cell adhesion under controlled physiological and pathological conditions for applications such as assessing materials for implant and replacement surgeries. They recently followed up on this work to use the DANI to study adhesion under physiological conditions, identifying conditions (*e.g.*, a temperature of 37°C and pH of 74) where was adhesion was favorable or detachment promoted.[192] Bussonnière et al.[193] and Sivanantha et al.[194] both applied this concept to use SAW-initiated cell de-adhesion as a method for cell separation and identification, with Bussonnière et al. separating human embryonic kidney (HEK 293) cells from, smooth muscle cells (A7r5) in a droplet and Sivanantha et al. applying the technique to healthy, treated, and malaria-infected red blood cells. The advantage with the SAW approach is that the method is inherently label-free and highly selective, without adversely affecting cell viability (Bussonnière et al. measured apoptosis rates less than 5%).

4. Perspectives and Directions for the Future

It is clear that research activity into SAW-based analytical techniques is very active, and the reasons are obvious – the potential for cheap, low-power, simple devices is great. However, they are still limited and gas sensors excepted, translation into commercial products continues to face barriers. Recent developments over the past several years, from the high selectivity of biosensors to the nearly-commercial atomization products for pulmonary drug delivery and mass spectrometry, suggest that we are likely at a tipping point, where the translation of SAW-based devices will quickly accelerate over the next few years. Additionally, fully-integrated packages that take advantage of the inherently small size of a SAW device – including miniaturized electronics, flexible substrate strategies, and integration with other analytical technologies – are close to being realized. Still, there are many opportunities to improve on SAW devices in the future.

As noted in Section 2, while SAW sensors for gas targets are now available commercially, SAW biosensors for molecular targets in liquid are not yet at a mature level.[18] The sensitivity of Love-mode and shear-horizontal SAW sensors for molecular targets in water, like protein and DNA, is exceedingly poor, with roughly μM to nM detection limits.[94,195] However, the potential impact of powerful sensors in the bioanalytical domain is significant, and it is in this area where there may be the most opportunity for future developments in SAW devices. We therefore focus on these applications as an area for future research. The relative insensitivity of SAW sensors is an issue that needs to be addressed moving forward, and simply modifying the sensing layer may produce incremental improvements but not the large advances the field requires. Earlier work on SAW DNA sensing from raw samples often required polymerase chain reaction (PCR) amplification, which requires extensive pretreatment by centrifugation and dialysis with heavy equipment and hence diminishes the portability or low-power advantage of a SAW sensor. Therefore, future attention should focus on improving sensitivity for the analysis of physiological fluids, without the need for other significant pre-treatment instruments.

To overcome this obstacle, integrating with other sensor and microfluidic techniques may be the path forward. For example, in contrast to SAW sensors, cantilever mechanical sensors exhibit single-molecule sensitivity but are extremely non-selective. Despite numerous attempts, cantilever sensors have yet to be commercialized for molecular sensing of physiological samples. Cantilever vibration does not introduce sufficiently large shear flow around the target-probe complex to enhance selectivity. SAW vibrations, in contrast, introduce both shear flow and a normal electric field that can enhance selectivity but because they propagate over a relatively long distance, their sensitivity is compromised. A hybrid design that places a cantilever sensor or any localized sensor above a SAW substrate may introduce both sensitivity and selectivity. Coupling of a plasmonic bow-tie or other nanostructured optical sensors with SAW may have similar advantages. The remaining challenge is to transport molecules to the small sensors without loss, and potentially using additional IDTs to induce acoustic streaming could fulfill this role. One advantage of SAW microfluidics is that it can be done at the droplet scale, which precludes the need for a flowing solution, which requires large volumes and introduces analyte loss. While this would be a microfabrication and design challenge, the potential for coupled SAW and non-SAW sensors and SAW-driven microfluidics is there.

Another design that may improve the sensitivity of SAW sensors, but without coupling to another sensor, is to insert a smaller SAW resonant cavity into its long propagating length. The propagating SAW travelling wave can possibly be designed to transport the molecules across the sensor cavity. SAW-driven, electric field-induced dielectrophoresis due to the resonantly trapped SAW waves at the cavity may be able to trap the molecules into the cavity from the propagating SAW waves over the cavity. Again, using droplet microfluidics, this could be done with a small batch sample without flow. This purely SAW design may then produce high selectivity and sensitivity in a batch sample.

Label- and probe-free identification of target molecules would be the ideal biosensing platform, and they are achievable, in principle, with spectroscopic techniques. One direction is coupling a SAW device in a probe-free spectroscopic design by integrating it with another

spectroscopic technique based on frequency or amplitude shift, such as a cantilever sensor, an impedance electrochemical sensor, a plasmonic (or other optical sensor), or a nanopore sensor with resonant frequencies that coincide with the SAW frequency. For example, it has been recently shown that ion enrichment and depletion dynamics in a nanopore sensor has a specific time scale that is related to the resistance-capacitance (RC) time of the nanopore due to ion or macroion migration/build-up under the electric field.[196] A properly tuned SAW frequency could potentially use its AC surface electric field to selectively concentrate certain molecules within the nanopore. Such dynamic concentration, as in isotachophoreis, is able to separate different molecules with different mobility.[99] The role of the SAW vibration would be to enhance the sensitivity of these other small (nanoscale) sensors, which are more selective and more robust because of their geometry. Coupling with other oscillators, whose frequencies can be tuned more easily than SAW, also suggests the possibility of SAW enhanced optical, plasmonic, and impedances spectroscopic studies of unknown molecules, which may eliminate the need for specific antibody or oligo probes. Going one step further, using SAW itself as the spectroscopic platform would preclude coupling to another spectroscopic technique, and recent studies that show acousto-photonic coupling[197,198], with energy transfer between acoustic and optical mechanisms, may hold the key for SAW-integrated spectroscopy.

As suggested above, perhaps the most promising future of SAW devices consist of fully integrated platforms that utilize SAW for all processes – from sample handling to detection – and this could be a direction the field heads in the future. For all the potential sensing techniques highlighted above, upstream SAW handling for separation or similar should be explored. For example, many of these can be connected to highly selective SAW microfluidic designs that can remove debris and non-targets, making analysis of physiological or lightly-treated physiological fluids possible. Even more expansive concepts should also be considered, such as coupling SAW with additional microfluidic processes. For example, the field introduced by the SAW could be coupled with an electrophoretic field to carry out two-dimensional or travelling-wave fractionation of molecules upstream of the sensing module. If such multiplex SAW chips show potential, one can even envision SAW-directed transport of analytes to different sensing modules on the same chip. That being said, the simplicity and small form factor of SAW devices remain some of their most attractive features. But due to the wettability of microfluidic channels, liquid samples are highly contaminating, and hence each chip should be disposed after each sample. Given the expense of fabricating SAW substrates, SAW sensors for disposable chips can only be justified if they provide additional functionalities such as the ones suggested above. Alternatively, the SAW substrate could be isolated from the microfluidic circuits and can be detached after each use.

5. Final Thoughts

In both the near-term and the long-term, the maturation and evolution of SAW devices for chemical analysis will be an exciting field to both work in and follow. With many technologies close to realizing their full potential, and many more strategies still in their infancy, the field is an area that will continue to see exciting growth. In this review, we have attempted to highlight the wide variety of ways that SAW devices are currently being used

for chemical analysis and how the field can continue to grow in the future. With the ongoing pressing need for more sensitive, more selective, and more cost-effective analytical technologies, SAW technologies have the opportunity to make major inroads and become a major player in the field.

Acknowledgments

D.B.G., Z.R., and H.-C.C. acknowledge the support of NIH Grant HG009010-01.

References

1. White R, Voltmer F. Applied physics letters. 1965; 7:314–316.
2. Morgan, D. Surface acoustic wave filters: With applications to electronic communications and signal processing. Academic Press; 2010.
3. Morgan DP. International journal of high speed electronics and systems. 2000; 10:553–602.
4. Rocha-Gaso M-I, March-Iborra C, Montoya-Baides Á, Arnau-Vives A. Sensors. 2009; 9:5740–5769. [PubMed: 22346725]
5. Länge K, Rapp BE, Rapp M. Analytical and bioanalytical chemistry. 2008; 391:1509–1519. [PubMed: 18265962]
6. Jakubik WP. Thin Solid Films. 2011; 520:986–993.
7. Gronewold TM. analytica chimica acta. 2007; 603:119–128. [PubMed: 17963831]
8. Afzal A, Iqbal N, Mujahid A, Schirhagl R. Analytica Chimica Acta. 2013; 787:36–49. [PubMed: 23830419]
9. Barani A, Paktinat H, Janmaleki M, Mohammadi A, Mosaddegh P, Fadaei-Tehrani A, Sanati-Nezhad A. Biosensors and Bioelectronics. 2016; 85:714–725. [PubMed: 27262557]
10. Ding X, Li P, Lin S-CS, Stratton ZS, Nama N, Guo F, Slotcavage D, Mao X, Shi J, Costanzo F. Lab on a Chip. 2013; 13:3626–3649. [PubMed: 23900527]
11. Yeo LY, Friend JR. Annual Review of Fluid Mechanics. 2014; 46:379–406.
12. Qi A, Yeo LY, Friend JR. Physics of Fluids. 2008; 20:074103.
13. Rayleigh L. Proceedings of the London Mathematical Society. 1885; 1:4–11.
14. Lamb H. Proc Roy Soc London, Ser A. 1917; 93:114–128.
15. Vellekoop MJ. Ultrasonics. 1998; 36:7–14.
16. Kwon Y, Roh Y. Ultrasonics. 2004; 42:409–411. [PubMed: 15047320]
17. Love, AEH. Some problems of geodynamics. Dover; 1967.
18. Gaso M, Jiménez Y, Francis LA, Arnau A. State of the art in biosensors—general aspects, InTech. 2013; 10:53077.
19. Shilton R, Tan MK, Yeo LY, Friend JR. Journal of Applied Physics. 2008; 104:014910.
20. Ding X, Lin S-CS, Kiraly B, Yue H, Li S, Chiang I-K, Shi J, Benkovic SJ, Huang TJ. Proceedings of the National Academy of Sciences. 2012; 109:11105–11109.
21. Jakoby B, Vellekoop MJ. Smart materials and structures. 1997; 6:668.
22. Gonzalez P, Rakowski M, San Segundo D, Severi S, De Meyer K, Witvrouw A. IEEE Electron Device Letters. 2012; 33:1204–1206.
23. Tigli O, Zaghloul ME. IEEE Transactions on Device and Materials Reliability. 2008; 8:705–713.
24. Wang QJ, Pflügl C, Andress WF, Ham D, Capasso F, Yamanishi M. Journal of Vacuum Science & Technology B: Microelectronics and Nanometer Structures Processing, Measurement, and Phenomena. 2008; 26:1848–1851.
25. Wohltjen H, Dessy R. Analytical Chemistry. 1979; 51:1458–1464.
26. Wohltjen H, Dessy R. Analytical Chemistry. 1979; 51:1465–1470.
27. Berger M, Welle A, Gottwald E, Rapp M, Länge K. Biosensors and Bioelectronics. 2010; 26:1706–1709. [PubMed: 20719493]

28. Sankaranarayanan SK, Singh R, Bhethanabotla VR. Journal of Applied Physics. 2010; 108:104507.
29. Grate JW. Chemical reviews. 2008; 108:726–745. [PubMed: 18220425]
30. Lim C, Wang W, Yang S, Lee K. Sensors and Actuators B: Chemical. 2011; 154:9–16.
31. Moore DS. Review of Scientific Instruments. 2004; 75:2499–2512.
32. Pandya HM, Sharma M, Nimal A, Rajesh K. J Environ Nanotechnol. 2013; 2:15–21.
33. Priya RB, Venkatesan T, Pandiyarajan G, Pandya HM. J Environ Nanotechnol. 2015; 4:15–22.
34. Bender F, Mohler RE, Ricco AJ, Josse F. Analytical chemistry. 2014; 86:1794–1799. [PubMed: 24392747]
35. Dewan N, Singh SP, Sreenivas K, Gupta V. Sensors and Actuators B: Chemical. 2007; 124:329–335.
36. Hong HS, Chung GS. Sensors and Actuators B: Chemical. 2014; 195:446–451.
37. Balashov SM, Balachova OV, Pavani Filho A, Bazetto MCQ, de Almeida MG. ECS Trans. 2012; 49:445–450.
38. Guo YJ, Zhang J, Zhao C, Ma JY, Pang HF, Hu PA, Placido F, Gibson D, Zu XT, Zu HY, Fu YQ. Materials Research Bulletin. 2013; 48:5058–5063.
39. Qi P, Vermesh O, Grecu M, Javey A, Wang Q, Dai H, Peng S, Cho KJ. Nano Letters. 2003; 3:347–351.
40. Wang B, Zhu LF, Yang YH, Xu NS, Yang GW. The Journal of Physical Chemistry C. 2008; 112:6643–6647.
41. Ramgir NS, Yang Y, Zacharias M. Small. 2010; 6:1705–1722. [PubMed: 20712030]
42. Lin Q, Li Y, Yang M. Analytica Chimica Acta. 2012; 748:73–80. [PubMed: 23021810]
43. Sil D, Hines J, Udeoyo U, Borguet E. ACS Applied Materials & Interfaces. 2015; 7:5709–5714. [PubMed: 25746067]
44. Wang ZL. Advanced Materials. 2000; 12:1295–1298.
45. Hu J, Odom TW, Lieber CM. Accounts of Chemical Research. 1999; 32:435–445.
46. Xuan W, He M, Meng N, He X, Wang W, Chen J, Shi T, Hasan T, Xu Z, Xu Y, Luo JK. Scientific Reports. 2014; 4:7206 1–9. [PubMed: 25425458]
47. Lee HJ, Namkoong K, Cho EC, Ko C, Park JC, Lee SS. Biosensors and Bioelectronics. 2009; 24:3120–3125. [PubMed: 19423329]
48. Lee HJ, Lee SS, Namkoong K, Ko C, Park JC. In IEEE Sensors. 2008:231–234.
49. Jiang Y, Tan CY, Tan SY, Wong MS, Chen YF, Zhang L, Yao K, Gan SK, Verma C, Tan YJ. Sensors and Actuators B: Chemical. 2015; 209:78–84.
50. Di Pietrantonio F, Benetti M, Cannata D, Verona E, Palla-Papavlu A, Dinca V, Dinescu M, Mattle T, Lippert T. Sensors and Actuators B: Chemical. 2012; 174:158–167.
51. Ho CK, Lindgren ER, Rawlinson KS, McGrath LK, Wright JL. Sensors. 2003; 3:236–247.
52. Sayago I, Fernández M, Fontecha J, Horrillo M, Vera C, Obieta I, Bustero I. Sensors and Actuators B: Chemical. 2012; 175:67–72.
53. Kuypers JH, Reindl LM, Tanaka S, Esashi M. ieee transactions on ultrasonics, ferroelectrics, and frequency control. 2008:55.
54. Anisimkim V, Penza M, Valentini A, Quaranta F, Vasanelli L. Sensors and Actuators B: Chemical. 1995; 23:197–201.
55. Wang W-S, Wu T-T, Chou T-H, Chen Y-Y. Nanotechnology. 2009; 20:135503. [PubMed: 19420502]
56. Matsuda T, Uchishiba H, Ikata O, Nishihara T, Satoh V. 1994
57. Staples E, Schoenwald J, Rosenfeld R, Hartmann C. 1974
58. Penza M, Cassano G. Sensors and Actuators B: Chemical. 2000; 68:300–306.
59. Atashbar M, Sadek A, Wlodarski W, Sriram S, Bhaskaran M, Cheng C, Kaner R, Kalantar-Zadeh K. Sensors and Actuators B: Chemical. 2009; 138:85–89.
60. Atashbar MZ, Bazuin BJ, Simpeh M, Krishnamurthy S. Sensors and Actuators B: Chemical. 2005; 111:213–218.

61. Plotner M, Berger O, Stab H, Fischer W-J, Konig P, Beyerlein D, Schwarz A. 2001
62. Sivaramakrishnan S, Rajamani R, Smith C, McGee K, Mann K, Yamashita N. Sensors and Actuators B: Chemical. 2008; 132:296–304.
63. Yasin F, Tye K, Reaz MBI. 2005
64. Levit N, Pestov D, Tepper G. Sensors and Actuators B: Chemical. 2002; 82:241–249.
65. Li D, Ma M. Sensors and Actuators B: Chemical. 2000; 69:75–84.
66. Penza M, Rossi R, Alvisi M, Aversa P, Cassano G, Suriano D, Benetti M, Cannata D, Di Pietrantonio F, Verona E. 2008
67. Hao H-C, Lin T-H, Chen M-C, Yao D-J. 2010
68. Raj VB, Nimal A, Parmar Y, Sharma M, Sreenivas K, Gupta V. Sensors and Actuators B: Chemical. 2010; 147:517–524.
69. Tang Y-L, Li Z-J, Ma J-Y, Guo Y-J, Fu Y-Q, Zu X-T. Sensors and Actuators B: Chemical. 2014; 201:114–121.
70. Tang Y-L, Li Z-J, Ma J-Y, Su H-Q, Guo Y-J, Wang L, Du B, Chen J-J, Zhou W, Yu Q-K. Journal of hazardous materials. 2014; 280:127–133. [PubMed: 25151235]
71. Meulendyk BJ, Wheeler MC, da Cunha MP. IEEE Sensors Journal. 2011; 11:1768–1775.
72. Raj VB, Singh H, Nimal A, Sharma M, Gupta V. Sensors and Actuators B: Chemical. 2013; 178:636–647.
73. http://ph.parker.com/us/17554/en/trihalomethane-thm-water-analyzer
74. https://ip.sandia.gov/technology.do/techID=83
75. http://biosensor.se/products
76. http://www.estcal.com
77. Ewing RG, Clowers BH, Atkinson DA. Analytical Chemistry. 2013; 85:10977–10983. [PubMed: 24090362]
78. McGill RA, Mlsna TE, Chung R, Nguyen VK, Stepnowski J. Sensors and Actuators B: Chemical. 2000; 65:5–9.
79. Inoue Y, Kato Y, Sato K. Journal of the Chemical Society, Faraday Transactions. 1992; 88:449–454.
80. Gizeli E, Goddard NJ, Lowe CR, Stevenson AC. Sensors and Actuators B: Chemical. 1992; 6:131–137.
81. Gizeli E, Stevenson AC, Goddard NJ, Lowe CR. Sensors and Actuators B: Chemical. 1993; 14:638–639.
82. Kondoh J, Matsui Y, Shiokawa S. Japanese journal of applied physics. 1993; 32:2376.
83. Kondoh J, Muramatsu T, Nakanishi T, Matsui Y, Shiokawa S. Sensors and Actuators B: Chemical. 2003; 92:191–198.
84. Ramshani Z, Reddy AS, Narakathu BB, Wabeke JT, Obare SO, Atashbar MZ. Sensors and Actuators B: Chemical. 2015; 217:72–77.
85. Verma P, Yadava R. Sensors and Actuators B: Chemical. 2015; 209:751–769.
86. Onen O, Sisman A, Gallant ND, Kruk P, Guldiken R. Sensors. 2012; 12:7423–7437. [PubMed: 22969352]
87. Tretjakov A, Syritski V, Reut J, Boroznjak R, Oepik A. Analytica chimica acta. 2016; 902:182–188. [PubMed: 26703269]
88. Liu X, Wang J-Y, Mao X-B, Ning Y, Zhang G-J. Analytical chemistry. 2015; 87:9352–9359. [PubMed: 26316457]
89. Chang K, Pi Y, Lu W, Wang F, Pan F, Li F, Jia S, Shi J, Deng S, Chen M. Biosensors and Bioelectronics. 2014; 60:318–324. [PubMed: 24836014]
90. Kim YW, Meyer MT, Berkovich A, Subramanian S, Iliadis AA, Bentley WE, Ghodssi R. Sensors and Actuators A: Physical. 2016; 238:140–149.
91. Li D, Feng Y, Zhou L, Ye Z, Wang J, Ying Y, Ruan C, Wang R, Li Y. Analytica chimica acta. 2011; 687:89–96. [PubMed: 21241851]
92. Wang T, Green R, Nair RR, Howell M, Mohapatra S, Guldiken R, Mohapatra SS. Sensors. 2015; 15:32045–32055. [PubMed: 26703604]

93. Matatagui D, Fontecha JL, Fernández MJ, Gràcia I, Cané C, Santos JP, Horrillo MC. Sensors. 2014; 14:12658–12669. [PubMed: 25029282]
94. Puiu M, Gurban A-M, Rotariu L, Brajnicov S, Viespe C, Bala C. Sensors. 2015; 15:10511–10525. [PubMed: 25951337]
95. Csete M, Hunt WD. Journal of clinical monitoring and computing. 2013; 27:427–431. [PubMed: 23471596]
96. Chang K, Wang F, Ding Y, Pan F, Li F, Jia S, Lu W, Deng S, Shi J, Chen M. Biosensors and Bioelectronics. 2014; 54:151–157. [PubMed: 24269758]
97. Taller D, Richards K, Slouka Z, Senapati S, Hill R, Go DB, Chang H-C. Lab on a Chip. 2015; 15:1656–1666. [PubMed: 25690152]
98. Groneworkd TM, Baumgartner A, Quandt E, Famulok M. Analytical Chemistry. 2006; 78:4865–4871. [PubMed: 16841904]
99. Marczak S, Senapati S, Slouka Z, Chang H-C. Biosensors and Bioelectronics. 2016; 86:840. [PubMed: 27494807]
100. Cheng I-F, Senapati S, Cheng S, Basuray S, Chang H-C, Chang H-C. Lab on a Chip. 2010; 10:828–831. [PubMed: 20379565]
101. Basuray S, Senapati S, Aijian A, Mahon AR, Chang H-C. ACS Nano. 2009; 3:1823. [PubMed: 19583249]
102. Jin H, Zhou J, He X, Wang W, Guo H, Dong S, Wang D, Xu Y, Geng J, Luo J. Scientific reports. 2013; 3:2140. [PubMed: 23828169]
103. Li Q, Liu H, Li G, Zeng F, Pan F, Luo J, Qian L. Journal of Electronic Materials. 2016; 45:2702–2709.
104. Roshanghias A, Krivec M, Bardong J, Abram A, Binder A. 2016
105. Cenni F, Cazalbou J, Mir S, Rufer L. Microelectronics Journal. 2010; 41:723–732.
106. Alghane M, Chen B, Fu YQ, Li Y, Luo J, Walton A. Journal of Micromechanics and Microengineering. 2010; 21:015005.
107. Rambach RW, Taiber J, Scheck CML, Meyer C, Reboud J, Cooper JM, Franke T. Scientific Reports. 2016; 6:24962. [PubMed: 27174539]
108. Rezk AR, Manor O, Friend JR, Yeo LY. Nature communications. 2012; 3:1167.
109. Tan MK, Friend JR, Yeo LY. Physical Review Letters. 2009; 103:024501. [PubMed: 19659210]
110. Rezk AR, Qi A, Friend JR, Li WH, Yeo LY. Lab on a Chip. 2012; 12:773–779. [PubMed: 22193520]
111. Taller D, Go DB, Chang H-C. Physical Review E. 2013; 87:053004.
112. Taller D, Go DB, Chang H-C. Physical Review Letters. 2012; 109:224301. [PubMed: 23368125]
113. Cheng L-J, Chang H-C. Biomicrofluidics. 2011; 5:046502.
114. Heron SR, Wilson R, Shaffer SA, Goodlett DR, Cooper JM. Analytical Chemistry. 2010; 82:3985–3989. [PubMed: 20364823]
115. Ho J, Tan MK, Go DB, Yeo LY, Friend JR, Chang H-C. Analytical Chemistry. 2011; 83:3260–3266. [PubMed: 21456580]
116. Mitsakakis K, Tserepi A, Gizeli E. Microelectronic Engineering. 2009; 86:1416–1418.
117. Bourquin Y, Reboud J, Wilson R, Cooper JM. Lab on a Chip. 2010; 10:1898–1901. [PubMed: 20535420]
118. Shilton RJ, Glass NR, Chan P, Yeo LY, Friend JR. Applied Physics Letters. 2011; 98:254103.
119. Schmid L, Wixforth A, Weitz DA, Franke T. Microfluidics and Nanofluidics. 2012; 12:229–235.
120. Matatagui D, Moynet D, Fernández MJ, Fontecha J, Esquivel JP, Gràcia I, Cané C, Déjous C, Rebière D, Santos JP, Horrillo MC. Sensors and Actuators B: Chemical. 2013; 185:218–224.
121. Shilton RJ, Travagliati M, Beltram F, Cecchini M. Advanced Materials. 2014; 26:4941–4946. [PubMed: 24677370]
122. Shilton RJ, Mattoli V, Travagliati M, Agostini M, Desii A, Beltram F, Cecchini M. Advanced Functional Materials. 2015; 25:5895–5901.
123. Riaud A, Baudoin M, Thomas JL, Matar OB. IEEE Transactions on Ultrasonics, Ferroelectrics, and Frequency Control. 2016; 63:1601–1607.

124. Luo JT, Geraldi NR, Guan JH, McHale G, Wells GG, Fu YQ. Physical Review Applied. 2017; 7:014017.
125. Chono K, Shimizu N, Matsui Y, Kondoh J, Shiokawa S. Japanese Journal of Applied Physics. 2004; 43:2987.
126. Kim J-W, Yamagata Y, Takasaki M, Lee B-H, Ohmori H, Higuchi T. Sensors and Actuators B: Chemical. 2005; 107:535–545.
127. Kurosawa M, Watanabe T, Futami A, Higuchi T. Sensors and Actuators A: Physical. 1995; 50:69–74.
128. Ang KM, Yeo LY, Hung YM, Tan MK. Lab on a Chip. 2016; 16:3503–3514. [PubMed: 27502324]
129. Rezk AR, Tan JK, Yeo LY. Advanced materials. 2016; 28:1970–1975. [PubMed: 26743122]
130. Winkler A, Harazim S, Collins D, Brünig R, Schmidt H, Menzel S. Biomedical Microdevices. 2017; 19:9. [PubMed: 28127655]
131. Ang KM, Yeo LY, Friend JR, Hung YM, Tan MK. Journal of Aerosol Science. 2015; 79:48–60.
132. Kirchner A, Winkler A, Menzel S, Holzapfel B, Hühne R. IEEE Transactions on Applied Superconductivity. 2016; 26:1–4.
133. Winkler A, Kirchner A, Bergelt P, Hühne R, Menzel S. Journal of Sol-Gel Science and Technology. 2016; 78:26–33.
134. Anand S, Nylk J, Neale SL, Dodds C, Grant S, Ismail MH, Reboud J, Cooper JM, McGloin D. Optics Express. 2013; 21:30148. [PubMed: 24514593]
135. Qi A, Friend JR, Yeo LY, Morton DA, McIntosh MP, Spiccia L. Lab on a Chip. 2009; 9:2184–2193. [PubMed: 19606295]
136. Rajapaksa A, Qi A, Yeo LY, Coppel R, Friend JR. Lab on a Chip. 2014; 14:1858–1865. [PubMed: 24740643]
137. Cortez-Jugo C, Qi A, Rajapaksa A, Friend JR, Yeo LY. Biomicrofluidics. 2015; 9:052603. [PubMed: 25945147]
138. Rajapaksa AE, Ho JJ, Qi A, Bischof R, Nguyen T-H, Tate M, Piedrafita D, McIntosh MP, Yeo LY, Meeusen E. Respiratory research. 2014; 15:60. [PubMed: 24884387]
139. Wang Y, Rezk AR, Khara JS, Yeo LY, Ee PLR. Biomicrofluidics. 2016; 10:034115. [PubMed: 27375820]
140. Alhasan L, Qi A, Rezk AR, Yeo LY, Chan PP. Integrative Biology. 2016; 8:12–20. [PubMed: 26611725]
141. Qi A, Yeo L, Friend J, Ho J. Lab on a Chip. 2010; 10:470–476. [PubMed: 20126687]
142. Huang Y, Yoon SH, Heron SR, Masselon CD, Edgar JS, Tureček F, Goodlett DR. Journal of The American Society for Mass Spectrometry. 2012; 23:1062–1070. [PubMed: 22476889]
143. Hommersom B, Syed SU, Eijkel GB, Kilgour D, Goodlett DR, Heeren R. Rapid Communications in Mass Spectrometry. 2016; 30:352–358. [PubMed: 26754127]
144. Yoon SH, Huang Y, Edgar JS, Ting YS, Heron SR, Kao Y, Li Y, Masselon CD, Ernst RK, Goodlett DR. Analytical chemistry. 2012; 84:6530–6537. [PubMed: 22742654]
145. Yoon SH, Liang T, Schneider T, Oyler BL, Chandler CE, Ernst RK, Yen GS, Huang Y, Nilsson E, Goodlett DR. Rapid Communications in Mass Spectrometry. 2016; 30:2555–2560.
146. Huang Y, Heron SR, Clark AM, Edgar JS, Yoon SH, Kilgour D, Turecek F, Aliseda A, Goodlett DR. Journal of Mass Spectrometry. 2016; 51:424–429. [PubMed: 27270865]
147. Monkkonen L, Edgar JS, Winters D, Heron SR, Mackay CL, Masselon CD, Stokes AA, Langridge-Smith PR, Goodlett DR. Journal of Chromatography A. 2016; 1439:161–166. [PubMed: 26826755]
148. Yen GS, Edgar JS, Yoon SH, Huang Y, Heron SR, Chiu DT, Goodlett DR. Rapid Communications in Mass Spectrometry. 2016; 30:1096–1100. [PubMed: 27003047]
149. Tveen-Jensen K, Gesellchen F, Wilson R, Spickett CM, Cooper JM, Pitt AR. Scientific reports. 2015:5.
150. Alvarez M, Friend JR, Yeo LY. Langmuir. 2008; 24:10629–10632. [PubMed: 18795809]

151. Shi J, Ahmed D, Mao X, Lin S-CS, Lawit A, Huang TJ. Lab on a Chip. 2009; 9:2890–2895. [PubMed: 19789740]
152. Shi J, Huang H, Stratton Z, Huang Y, Huang TJ. Lab on a Chip. 2009; 9:3354–3359. [PubMed: 19904400]
153. Chen Y, Wu M, Ren L, Liu J, Whitley PH, Wang L, Huang TJ. Lab on a Chip. 2016; 16:3466–3472. [PubMed: 27477388]
154. Ding X, Peng Z, Lin S-CS, Geri M, Li S, Li P, Chen Y, Dao M, Suresh S, Huang TJ. Proceedings of the National Academy of Sciences. 2014; 111:12992–12997.
155. Guo F, Mao Z, Chen Y, Xie Z, Lata JP, Li P, Ren L, Liu J, Yang J, Dao M. Proceedings of the National Academy of Sciences. 2016; 113:1522–1527.
156. Guo F, Zhou W, Li P, Mao Z, Yennawar NH, French JB, Huang TJ. small. 2015; 11:2733–2737. [PubMed: 25641793]
157. Lata JP, Guo F, Guo J, Huang PH, Yang J, Huang TJ. Advanced Materials. 2016; 28:8632–8638. [PubMed: 27571239]
158. Li P, Mao Z, Peng Z, Zhou L, Chen Y, Huang P-H, Truica CI, Drabick JJ, El-Deiry WS, Dao M. Proceedings of the National Academy of Sciences. 2015; 112:4970–4975.
159. Li S, Ma F, Bachman H, Cameron CE, Zeng X, Huang TJ. Journal of Micromechanics and Microengineering. 2016; 27:015031. [PubMed: 28798539]
160. Li S, Ren L, Huang P-H, Yao X, Cuento RA, McCoy JP, Cameron CE, Levine SJ, Huang TJ. Analytical chemistry. 2016; 88:5655–5661. [PubMed: 27183317]
161. Nawaz AA, Chen Y, Nama N, Nissly RH, Ren L, Ozcelik A, Wang L, McCoy JP, Levine SJ, Huang TJ. Analytical chemistry. 2015; 87:12051–12058. [PubMed: 26331909]
162. Ren L, Chen Y, Li P, Mao Z, Huang P-H, Rufo J, Guo F, Wang L, McCoy JP, Levine SJ. Lab on a Chip. 2015; 15:3870–3879. [PubMed: 26289231]
163. Collins DJ, Morahan B, Garcia-Bustos J, Doerig C, Plebanski M, Neild A. Nature communications. 2015:6.
164. Witte C, Reboud J, Wilson R, Cooper JM, Neale SL. Lab on a Chip. 2014; 14:4277. [PubMed: 25224539]
165. Destgeer G, Jung JH, Park J, Ahmed H, Sung HJ. Analytical Chemistry. 2016
166. Ma Z, Collins DJ, Guo J, Ai Y. Analytical Chemistry. 2016; 88:11844–11851. [PubMed: 27934119]
167. Li H, Friend JR, Yeo LY. Biomedical microdevices. 2007; 9:647–656. [PubMed: 17530412]
168. Tan MK, Friend JR, Yeo LY. Lab on a Chip. 2007; 7:618–625. [PubMed: 17476381]
169. Ang KM, Yeo LY, Hung YM, Tan MK. Biomicrofluidics. 2016; 10:054106. [PubMed: 27703592]
170. Raghavan RV, Friend JR, Yeo LY. Microfluidics and Nanofluidics. 2010; 8:73.
171. Rogers PR, Friend JR, Yeo LY. Lab on a Chip. 2010; 10:2979–2985. [PubMed: 20737070]
172. Glass NR, Shilton RJ, Chan PP, Friend JR, Yeo LY. small. 2012; 8:1881–1888. [PubMed: 22488691]
173. Kulkarni KP, Ramarathinam SH, Friend J, Yeo L, Purcell AW, Perlmutter P. Lab on a Chip. 2010; 10:1518–1520. [PubMed: 20517556]
174. Alhasan L, Qi A, Al-Abboodi A, Rezk A, Chan PP, Iliescu C, Yeo LY. ACS Biomaterials Science & Engineering. 2016; 2:1013–1022.
175. Saiki T, Utsumi Y. IEEJ Transactions on Electronics, Information and Systems. 2012; 132:70–76.
176. Saiki T, Utsumi Y. Electronics and Communications in Japan. 2014; 97:54–61.
177. Gracioso Martins AM, Glass NR, Harrison S, Rezk AR, Porter NA, Carpenter PD, Du Plessis J, Friend JR, Yeo LY. Analytical chemistry. 2014; 86:10812–10819. [PubMed: 25275830]
178. Chen Y, Nawaz AA, Zhao Y, Huang P-H, McCoy JP, Levine SJ, Wang L, Huang TJ. Lab on a Chip. 2014; 14:916–923. [PubMed: 24406848]
179. Mao Z, Li P, Wu M, Bachman H, Mesyngier N, Guo X, Liu S, Costanzo F, Huang TJ. ACS nano. 2017
180. Westerhausen C, Schnitzler LG, Wendel D, Krzyszton R, Lachelt U, Wagner E, Radler JO, Wixforth A. Micromachins. 2016; 7:150.

181. Zhang A-L, Wu Z-Q, Xia X-H. Talanta. 2011; 84:293–297. [PubMed: 21376947]
182. Ramesan S, Rezk AR, Cheng KW, Chan PP, Yeo LY. Lab on a Chip. 2016; 16:2820–2828. [PubMed: 27334420]
183. Lyford T, Millard P, da Cunha MP. 2012
184. Wilson R, Reboud JJ, Bourquin Y, Neale SL, Zhang Y, Cooper JM. Lab on a Chip. 2011; 11:323. [PubMed: 21057690]
185. Reboud J, Wilson R, Zhang Y, Ismail MH, Bourquin Y, Cooper JM. Lab on a Chip. 2012; 12:1268. [PubMed: 22327572]
186. Bourquin Y, Wilson R, Zhang Y, Reboud J, Cooper JM. Advanced Materials. 2011; 23:1458. [PubMed: 21433113]
187. Reboud J, Bourquin Y, Wilson R, Pall GS, Jiwaji M, Pitt AR, Graham A, Waters AP, Cooper JM. Proceedings of the National Academy of Sciences. 2012; 109:15162–15167.
188. Salehi-Reyhani A, Gesellchen F, Mampallil D, Wilson R, Reboud J, Ces O, Willison KR, Cooper JM, Klug DR. Analytical chemistry. 2015; 87:2161–2169. [PubMed: 25514590]
189. Taller D, Richards K, Slouka Z, Senapati S, Hill R, Go DB, Chang H-C. Lab on a Chip. 2015; 15:1656–1666. [PubMed: 25690152]
190. Vlassov AV, Magdaleno S, Setterquist R, Conrad R. Biochimica et Biophysica Acta (BBA)-General Subjects. 2012; 1820:940–948. [PubMed: 22503788]
191. Hartmann A, Stamp M, Kmeth R, Buchegger S, Stritzker B, Saldamli B, Burgkart RR, Schneider MF, Wixforth A. Lab on a Chip. 2014; 14:542. [PubMed: 24292668]
192. Stamp MEM, Jotten AM, Kudella PW, Breyer D, Strobl FG, Gleislinger TM, Wixforth A, Westerhausen C. Diagnostics. 2016; 6:38.
193. Bussonnière A, Miron Y, Baudoin M, Matar OB, Grandbois M, Charette P, Renaudin A. Lab on a Chip. 2014; 14:3556. [PubMed: 25029952]
194. Sivanantha N, Ma C, Collins DJ, Sesen M, Brenker J, Coppel R, Neild A, Alan T. Applied Physics Letters. 2014; 105:103704.
195. Hur Y, Han J, Seon J, Pak YE, Roh Y. Sensors and Actuators A: Physical. 2005; 120:462–467.
196. Yan Y, Schiffbauer J, Yossifon G, Chang HC. The Journal of Chemical Physics. 2015; 143:224705. [PubMed: 26671394]
197. Bahl G, Kim KH, Lee W, Liu J, Fan X, Carmon T. Nature Communications. 2013; 4:1994.
198. Beugnot JC, Lebrun S, Pauliat G, Maillotte H, Laude V, Sylvestre T. Nature Communications. 2014; 5:5242.

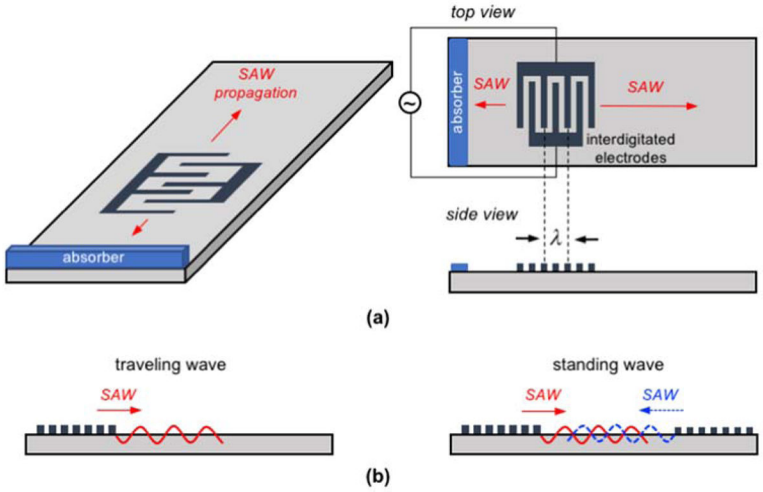

Fig. 1.

(a) Schematic of a single, planar IDT configuration, where the SAW propagates away from the IDT in both directions. Typically, an absorbent material such as a gel is used to inhibit reflection of the backward traveling SAW. The top and side views show a typical IDT structure with the interdigitated electrode fingers spaced $\lambda/2$. (b) Side views to two common actuation strategies. On the left is a traveling wave configuration, where a single IDT induces a SAW propagating away from the electrodes. Generally, the SAW propagates at the speed of sound of the crystal, which is typically ~10^3 m/s, but has an out-of-plane displacement amplitude of only ~10 nm. However, the displacement speed and acceleration can be very high, ~1 m/s and 10^5 m/s^2. On the right shows two sets of IDTs that generate counter-propagating SAWs. The SAWs interfere to form a standing wave.

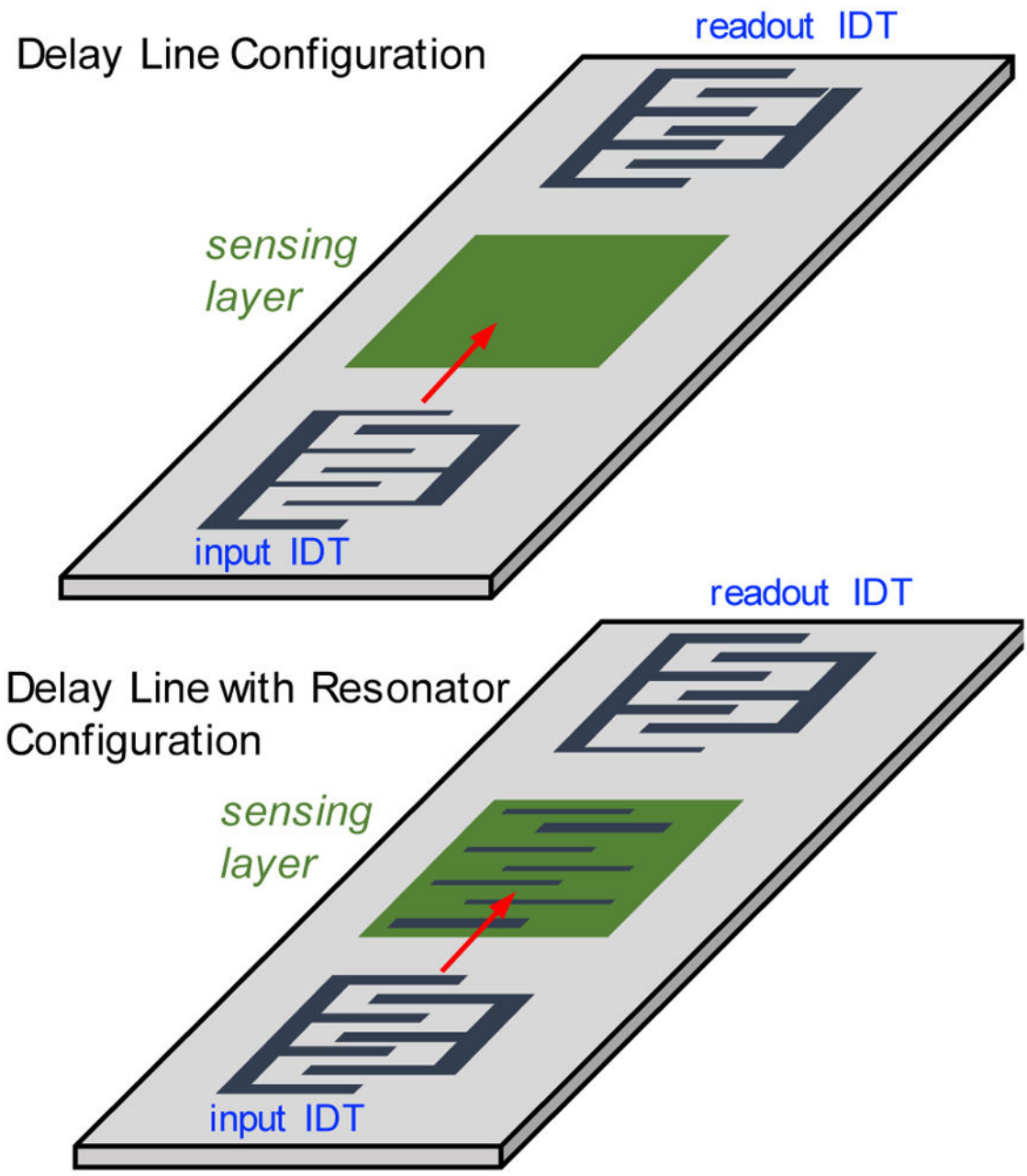

Fig. 2.

Two common configurations using a pair of IDTs for sensing applications. On the top is the delay line configuration, where a SAW is produced at the input IDT and as it travels through the sensing layer, interactions with adsorbed targets induce a frequency shift that can be detected at the readout IDT. On the bottom is a similar configuration but with additional IDT electrodes beneath the sensing layer. This resonator IDT acts as a reflector to set up a resonant cavity and increase sensitivity.

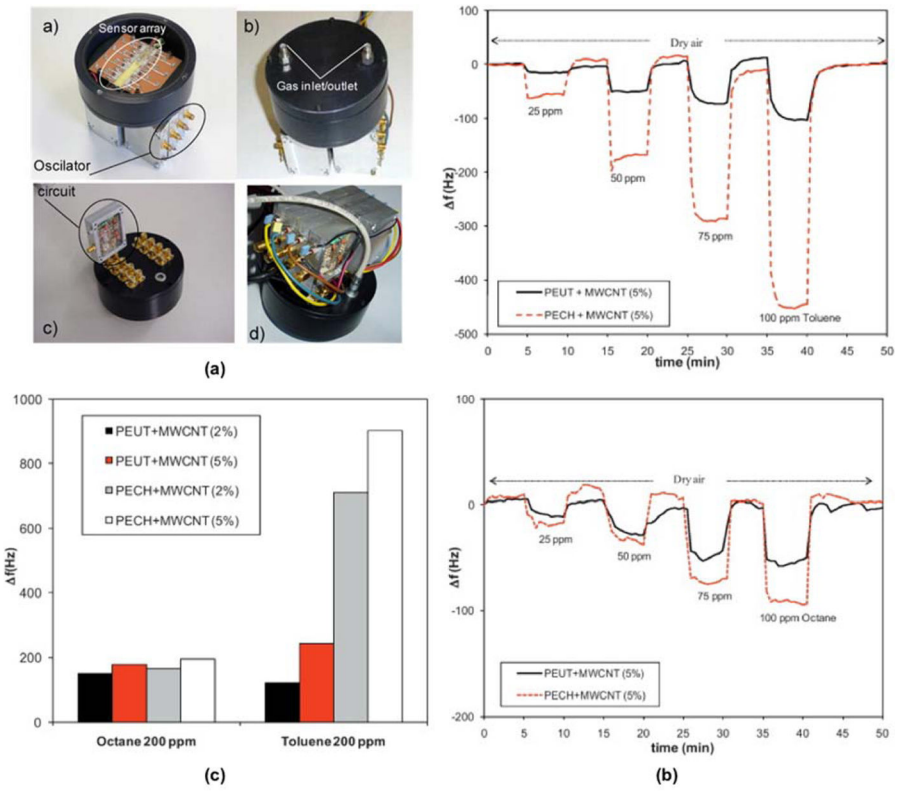

Fig. 3.

(a) The sensor array and testbed including oscillator circuits; a) and b) are the front view and c) and) are the back view. (b) Dynamic response to different concentrations of (top) octane and (bottom) toluene, at room temperature. (c) Sensor responses at 200 ppm to octane and toluene at room temperature. Adapted from Ref. [52] with permission from Elsevier.

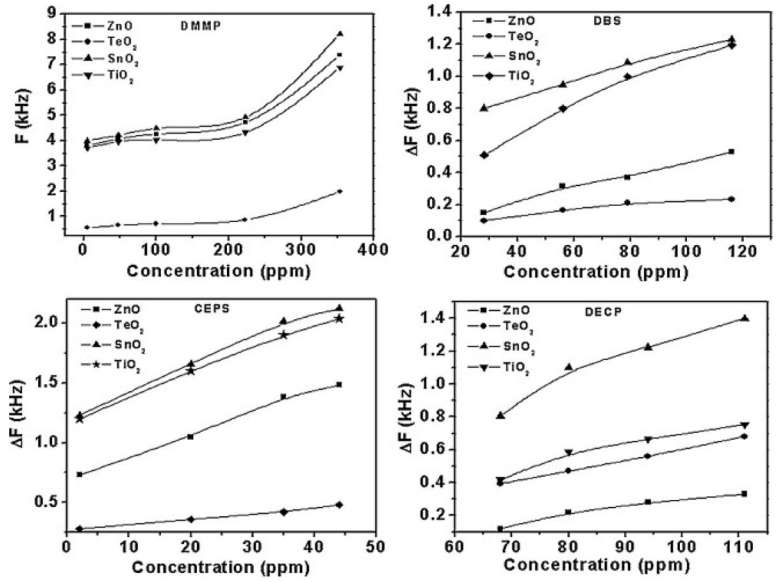

Fig. 4.

Variation in differential frequency shifts (*ΔF*) of SAW E-nose as a function of the concentration of different simulants of CWA on four different oxide sensing layers – ZnO, tellurium dioxide (TeO_2), tin dioxide (SnO_2), and titanium dioxide (TiO_2)). Upper left - dimethyl methyl phosphonate (DMMP), upper right - dibutyl sulfide (DBS), lower right - diethyl chlorophosphate (DECP), lower left - chloroethyl phenyl sulfide (CEPS). Adapted from Ref. [72] with permission from Elsevier.

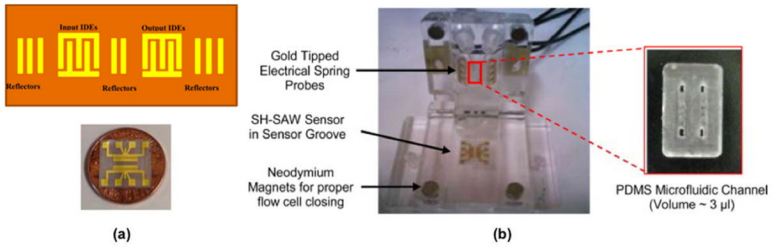

Fig. 5.

(a) Schematic of the SH-SAW device (top) and the as-fabricated SH-SAW sensor on a U.S. penny for reference (bottom). (b) Flow cell with the SH-SAW sensor in the sensor groove. (Inset: PDMS microfluidic flow channel). A chemical sensing layer, naphtho[2,3-a]dipyrido[3,2-h:2′,3′-f]phenazine-5,18-dione (QDPPZ), was synthesized and employed for the selective detection of lead nitrate ($PbNO_3$) and cadmium nitrate (CdNO) down to pM-level concentrations. Adapted from Ref. [84] with permission from Elsevier.

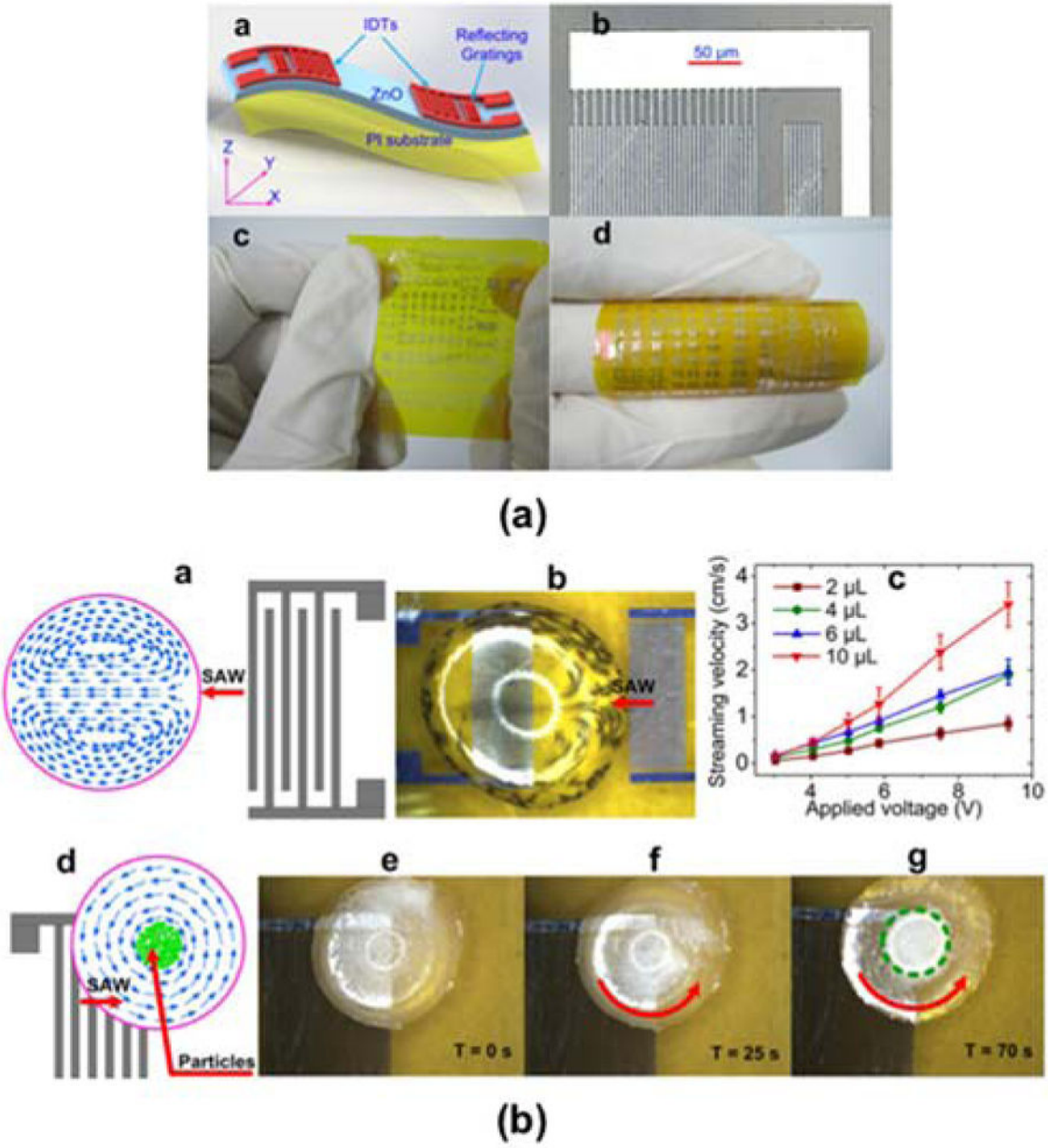

Fig. 6.

(a) Schematic of the flexible thin film ZnO/polyimide SAW devices and photographs of the IDT design and fabricated devices. (b) Schematics and photographs of induced acoustic streaming in a surface droplet along with measurements of the streamlining velocity as a function of the applied voltage and images showing the concentration of particles in the droplet. Adapted by permission from Macmillan Publishers Ltd: Ref. [103], 2013.

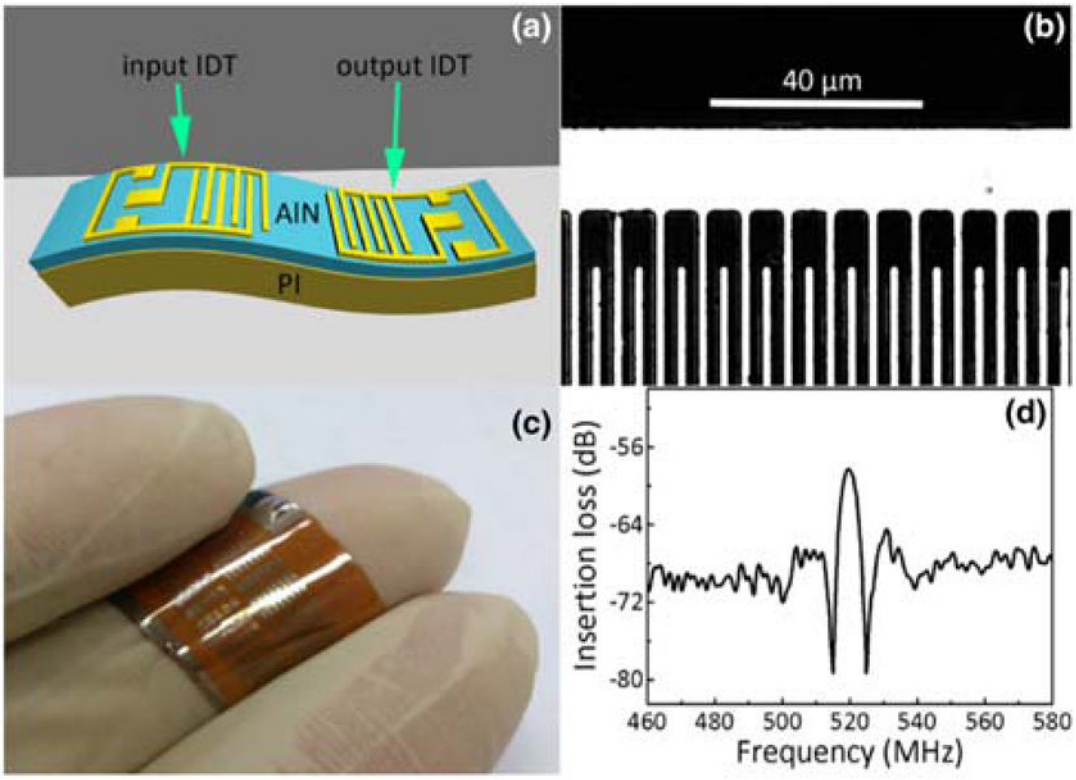

Fig. 7.

(a) Schematic of the developed flexible SAW delay line device on AlN/PI composite structure, (b) microscope image of interdigital transducer fingers, (c) photographs of flexible SAW delay line devices on PI substrate, and (d) frequency response of the flexible SAW delay line device. Used from Ref. [104] with permission of Springer.

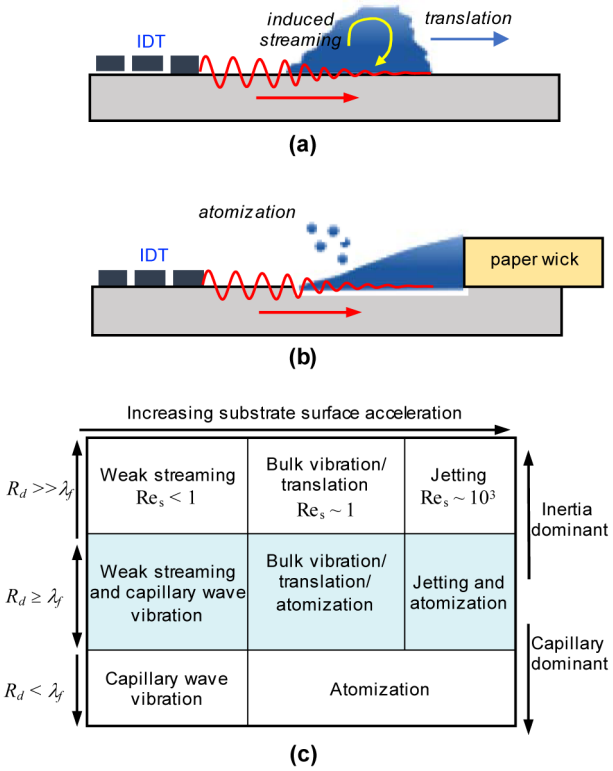

Fig. 8.

(a) Induced streaming due to the acoustic pressure of the refracted SAW wave into a surface droplet. In this traveling wave configuration, the droplet can translate or at sufficient SAW amplitude, break-up and be ejected from the surface. (b) A 'pinned' droplet configuration, where solution is fed from a paper wick connected to an external solution reservoir. A thin film of fluid is extracted from the wick onto the surface of the SAW device. Similar to the surface droplet configuration, at sufficient SAW amplitude the extracted film is atomized. (c) The modes of liquid break-up depending on the relative size of the droplet on the surface of the substrate (R_d) and the acoustic wavelength in the fluid (λ_f). The streaming Reynolds number (Re_s) is a non-dimensional number characterizing the inertia of the streaming fluid to viscous effects. Table adapted with permission from Ref. [109]. Copyrighted by the American Physical Society.

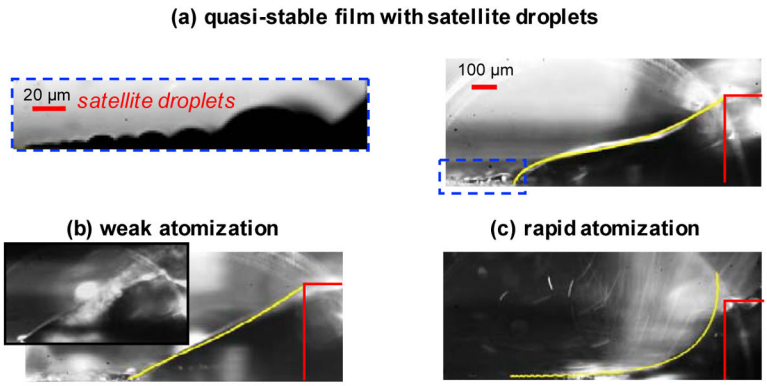

Fig. 9.

Film regimes under increasing SAW power from top to bottom for deionized (DI) water pumped through a paper wick on the surface of the SAW substrate. (a) Quasistable film regime (no atomization). The inset shows a zoomed view of the satellite surface droplets that form from the contact line of the extract thin film. (b) Weak atomization regime. Initial film rupture occurs and droplet emission takes place near the paper wick. The inset shows a discrete atomization event. (c) Rapid atomization regime, in which the film has thinned and aerosol emission occurs near the contact line. Numerical solutions corresponding to theory are overlaid in yellow and match the topology closely. The wicking paper is outlined in red on the right. The film regime figures are adapted with permission from Ref. 111. Copyrighted by the American Physical Society. The inset figure is adapted with permission from Ref. 112. Copyrighted by the American Physical Society.

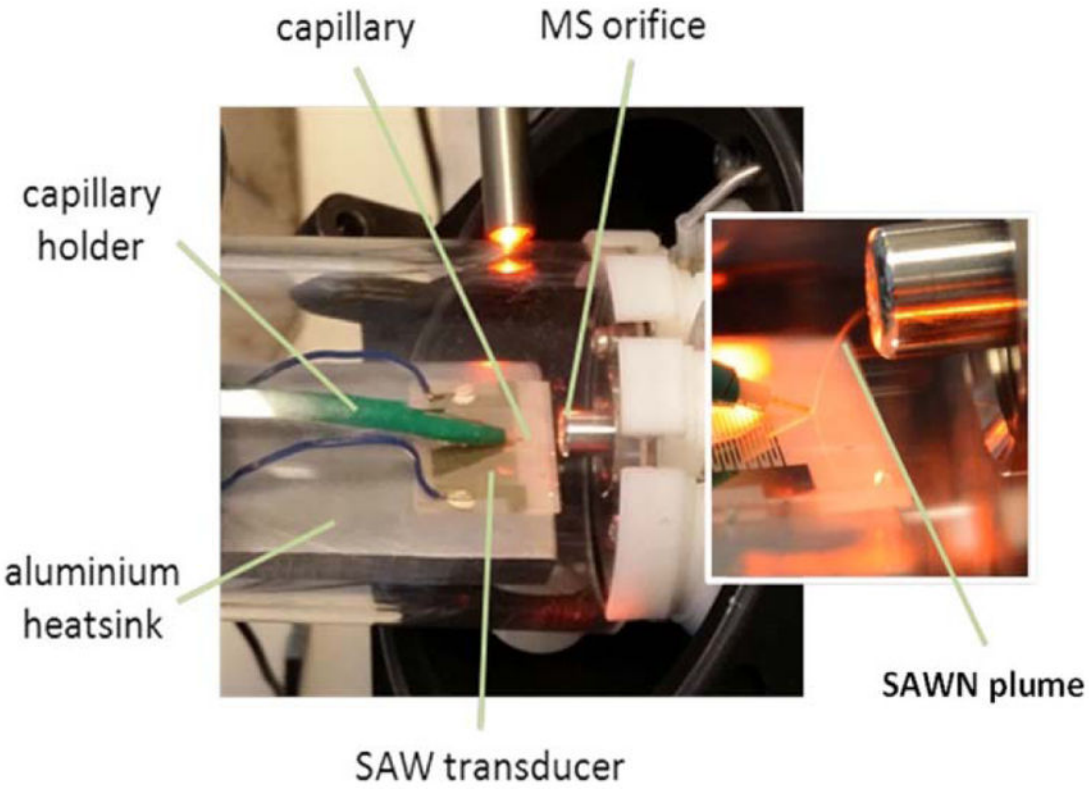

Fig. 10.

Photograph showing coupling of SAWN ionization device to LC capillary at the inlet of a mass spectrometer. Reproduced from Ref. [149] with permission from Wiley.

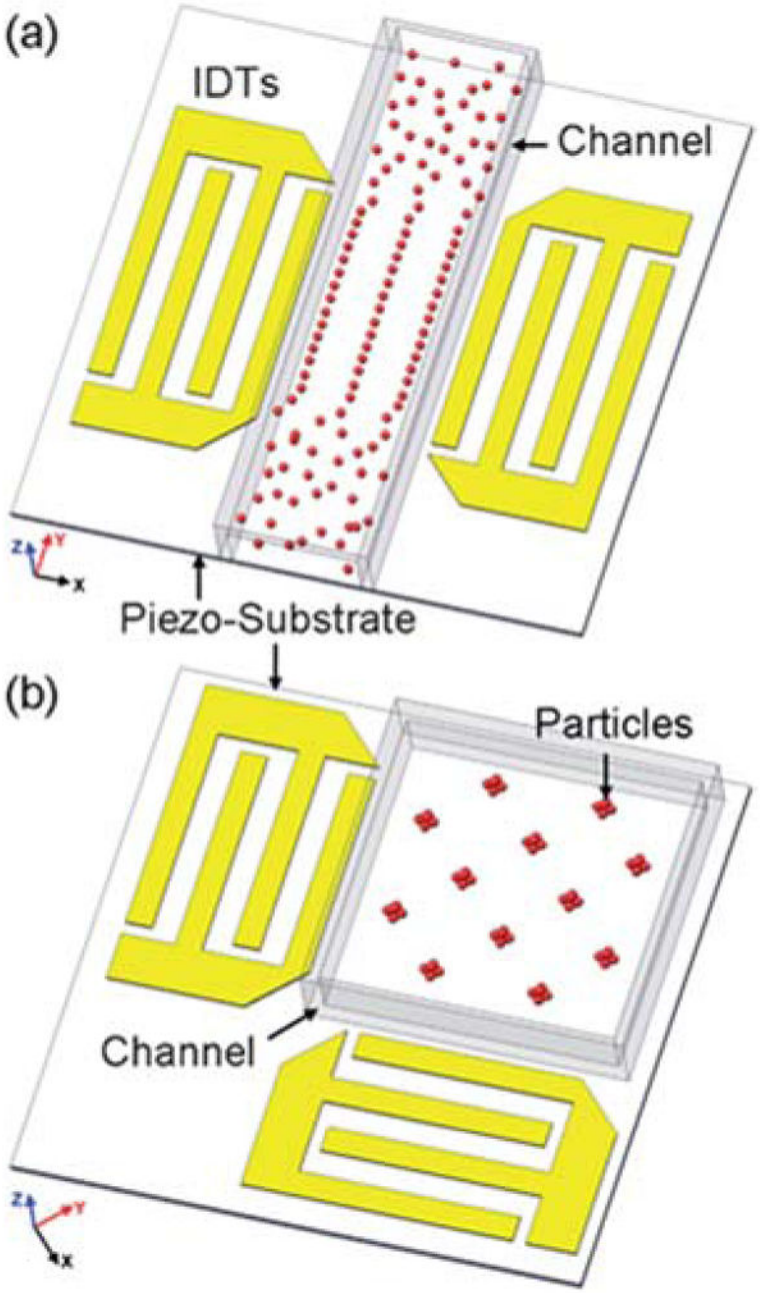

Fig. 11.

Schematic of the SSAW-based patterning devices. (a) 1D patterning using two parallel IDTs. (b) 2D patterning using two orthogonal IDTs (the angle between the IDTs can be changed to achieve different patterns). Reproduced from Ref. [151] with permission from The Royal Society of Chemistry.

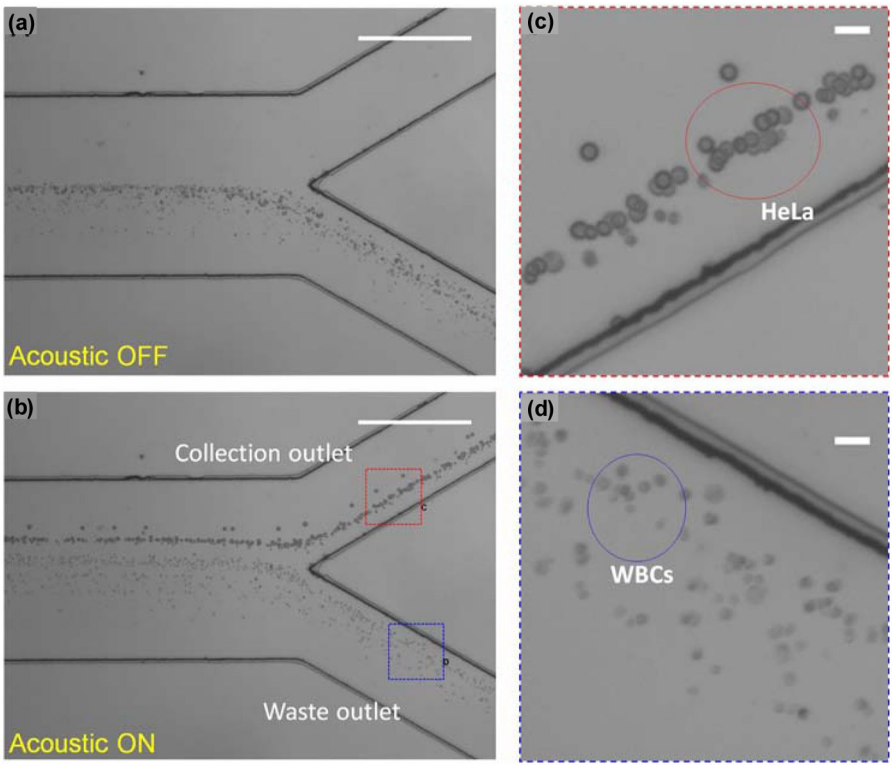

Fig. 12.

Micrographs of the separation process with acoustic field ON and OFF. (a) The mixture of HeLa cells and WBCs through a microfluidic channel with the acoustic field OFF. All of the cells were directed to the lower waste outlet by the hydrodynamic flow. No separation is observed. (b) When the acoustic field is ON, larger HeLa cells were pushed to the collection outlet, whereas the smaller WBCs still remained in the waste outlet. The separation between HeLa cells and WBCs can be observed. The stacked images are from 50 consecutive frames. (Scale bars, 515 μm.) (c and d) Zoomed-in images of the collection outlet and the waste outlet, respectively. (Scale bars, 30 μm.). Adapted from Ref. [158], courtesy National Academy of Sciences.

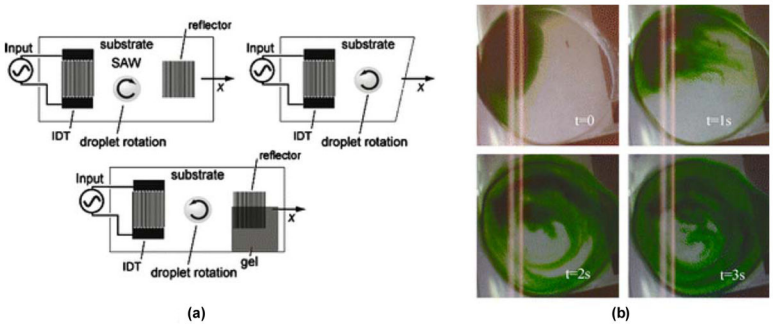

Fig. 13.

(a) Schemes for symmetry breaking of SAW propagation in order to generate azimuthal liquid recirculation. The left pictures shows one of the IDTs partly covered with α-gel damping material and the right picture shows the use of only one IDT with the wafer cut in a diagonal fashion. (b) Images at 60 frames/s showing the visualization of azimuthal bulk recirculation generated by asymmetric SAW propagation through dye streamlines induced by the flow. Adapted from Ref. [167] with permission of Springer.

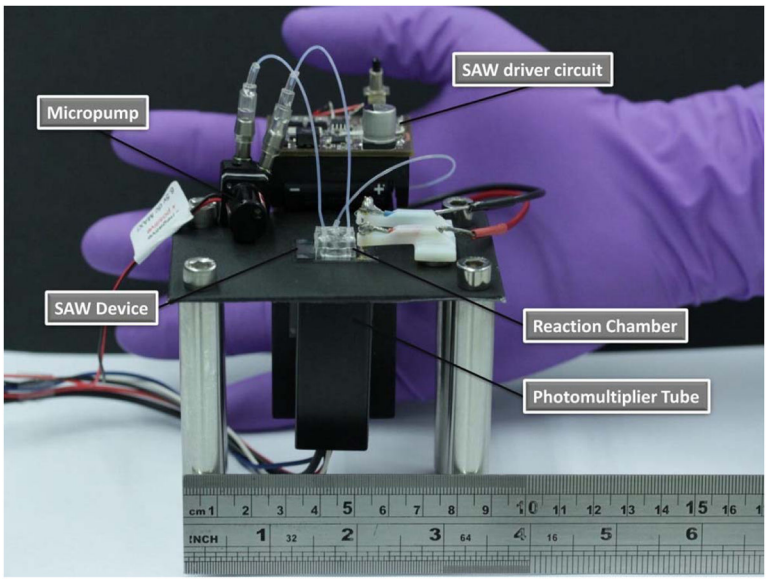

Fig. 14.

Image of the proposed portable FIA system which includes a micropump, the SAW chip powered by a miniature driver circuit that includes a signal generator and amplifier, the PDMS reaction chamber bonded to the chip and a portable photodetector, showing the possibility for complete integration and portability for field use. The total weight of the entire system is approximately 130 g. Reprinted with permission from Ref. [177]. Copyright 2014 American Chemical Society.

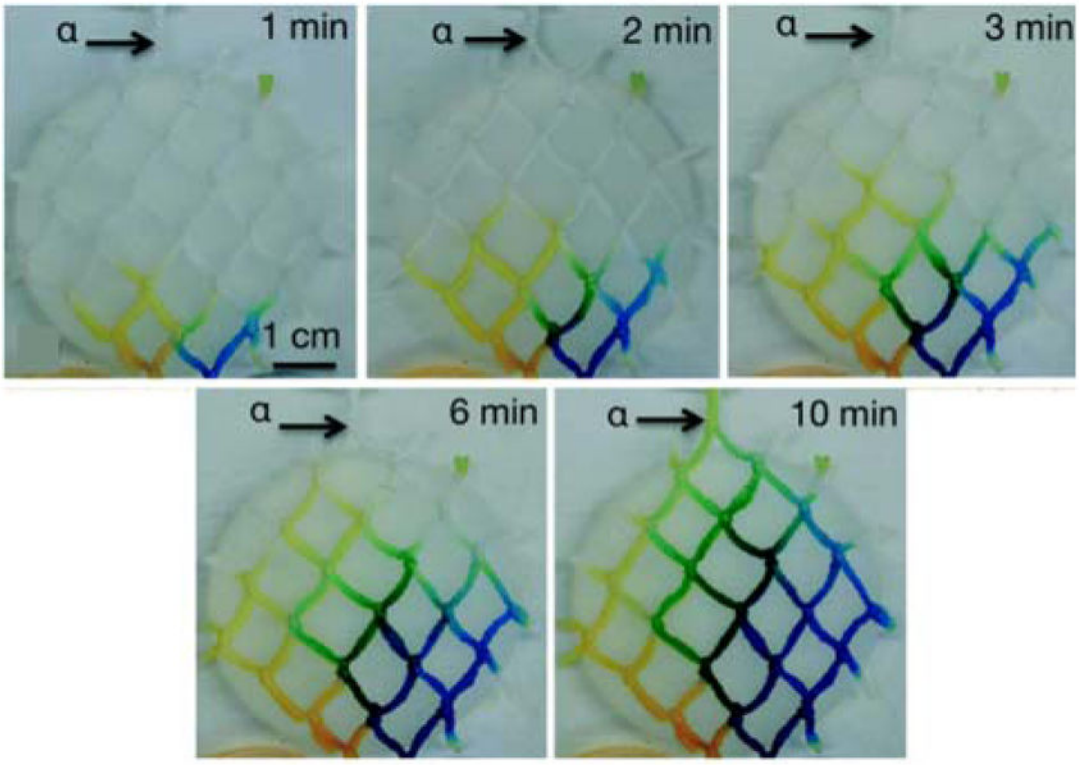

Fig. 15.

Time series images showing the transport and mixing of two colored solutions, yellow and blue, through the serial dilution and combinatorial thread network, drawn from the reservoirs at the bottom of the images (one inlet thread port was immersed in each reservoir) towards the outlet at location α when the SAW device placed at this location is activated. Due to the serial dilution and mixing, a stable symmetric concentration gradient across the network can be seen. Adapted from Ref. [182] with permission from The Royal Society of Chemistry.

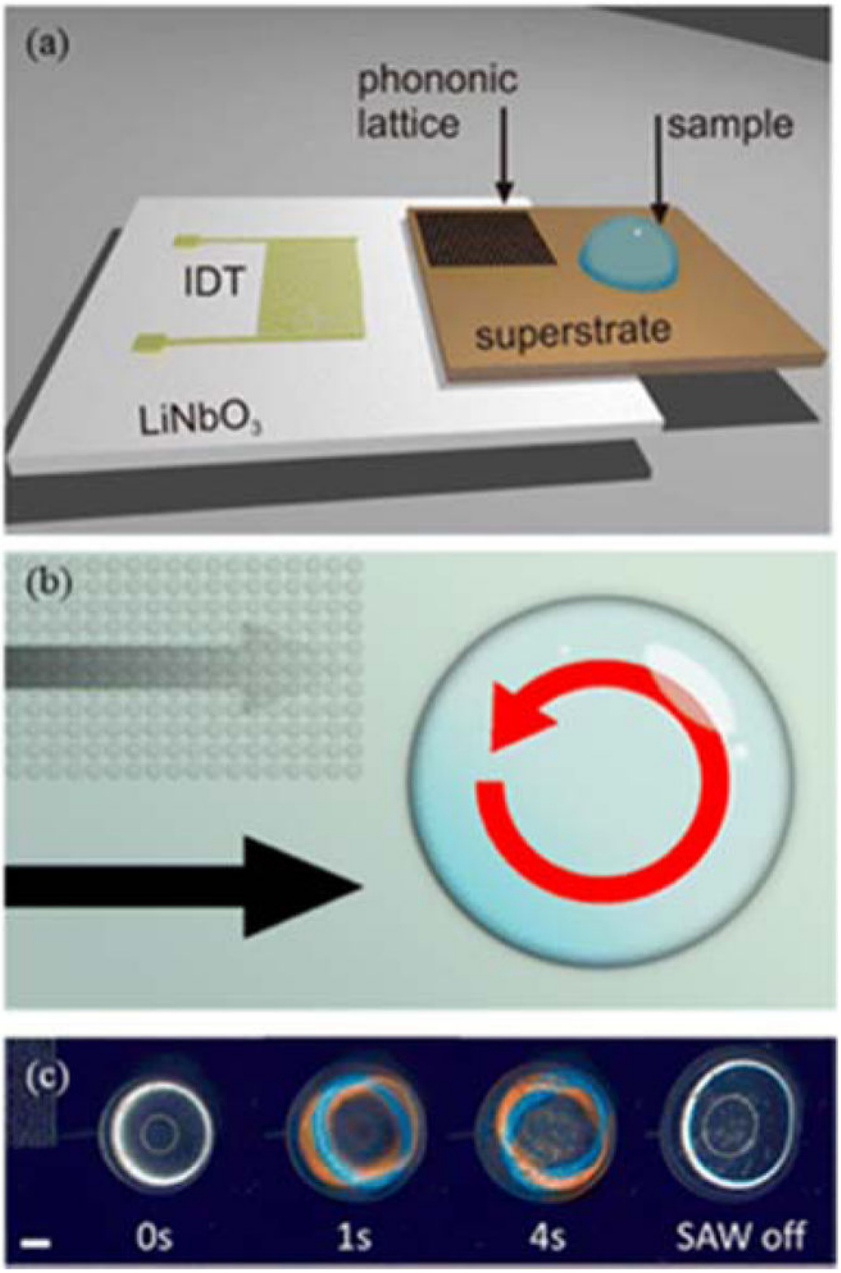

Fig. 16.

Surface acoustic wave (SAW) platform used to lyse cells. (a) Device architecture showing the interdigitated transducer (IDT) used to generate the SAW on the LiNbO3 piezoelectric wafer. The SAW is coupled into a phononic superstrate. A 20 μL droplet containing the cell suspension is deposited in the position shown. (b) The phononic lattice absorbs SAWs in a frequency-dependent manner. At ~ 10 MHz, propagation is hindered in region of the lattice, whereas it is unhindered in the adjacent region. This acts to create a rotational movement within the droplet and results in shear flows that contribute to the disruption of the cell membrane. (c) The sequence of images shows a droplet of cells undergoing SAW-induced mechanical lysis. The droplet containing cells has a cloudy appearance, which is observed to

become largely clear upon successful lysis of cells. Note that the colored rings observed in part of the image sequence are an optical effect of the stereomicroscope used to observe lysis. Scale bar 1 mm. Reprinted with permission from Ref. [188]. Copyright 2015 American Chemical Society.

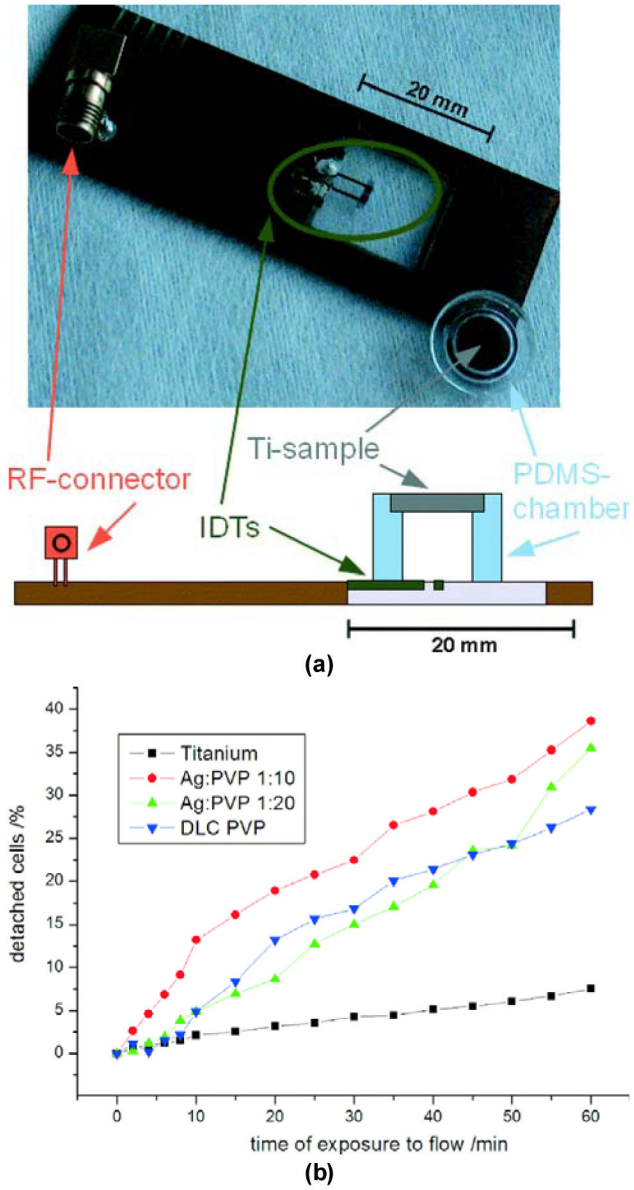

Fig. 17.

(a) Photograph (top) and schematic cross-section (bottom) of the setup for cell adhesion measurements. The system consists of a transparent piezoelectric LiNbO3 substrate with interdigital transducers (IDTs, green-brown color in the figure). On top of the substrate and the IDTs, a polydimethylsiloxane (PDMS)-chamber (blue) is placed which is covered by the implant specimen, in this case a titanium sample (grey). In the top photograph, the PDMS-chamber (upside-down) is removed from the LiNbO3 substrate, whereas the cross-section in the bottom part of the figure shows the system in its closed and assembled configuration. The electrical radio-frequency (rf) connector is labeled in orange. It is connected to the IDTs via silver conductive paste and two separated Cu-parts on the chip-carrier. (b) Percentage of detached SAOS-2 cells on different samples as marked by different symbols after 60 minutes of initial adhesion time versus time of flow exposure. Titanium exhibits the smallest de-

adhesion rate as compared to the different DLC surfaces. Within this set of substrates, the de-adhesion tendency increases with higher silver-doping. Reproduced from Ref. [191] with permission from The Royal Society of Chemistry.

Table 1

Comparison of SAW microfluidic devices.

Year	Author	Application	Frequency (MHz)	Structure
2009[116]	Mitsakakis et. al	Multi-channel microfluidic module for multi-analyte detection	155	Quartz/PMMA
2010[117]	Bourquin et. al	Fluid and particle manipulation	8–16	128° LiNbO3/Ti/Au
2011[118]	Shilton et. al	Rotational microfluidic motor	20	128° LiNbO3/Cr/Au,
2012[119]	Schmid et al.	Acoustic micropump	142	128° LiNbO3
2013[120]	Matatagui et. al	Pathogenic microorganism detection	163.2 and 159.7	ST-cut Quartz/Al
2014[121]	Shilton et al.	Nanoliter-droplet acoustic streaming	50, 100, 200, 400, 833, and 1250	128° LiNbO3/Ti/Au
2015[122]	Shilton et. al	Digital microfluidic heating	50, 100, 200, 400, 600, and 900	128° LiNbO3/Ti/Au
2016[123]	Riaud et. al	Versatile SAW toolbox for microfluidic applications	11.9	X-cut LiNbO3/Ti/Au
2017[124]	Luo et. al	Droplet Transportation	22.44	Si/ZnO/Al